

引用格式：王海洋，钟福军，潘家永，等，2025. 粤北澜河片麻状黑云母花岗岩的成因：锆石 U-Pb 年代学、Hf 同位素和地球化学约束[J]. 地质力学学报, 31(3): 539–556. DOI: 10.12090/j.issn.1006-6616.2024137

Citation: WANG H Y, ZHONG F J, PAN J Y, et al., 2025. Genesis of the gneissic biotite granite in Lanhe, northern Guangdong: Constraints from zircon U-Pb geochronology, Hf isotopes, and geochemistry[J]. Journal of Geomechanics, 31(3): 539–556. DOI: 10.12090/j.issn.1006-6616.2024137

粤北澜河片麻状黑云母花岗岩的成因：锆石 U-Pb 年代学、Hf 同位素和地球化学约束

王海洋^{1,2,3}, 钟福军^{1,2}, 潘家永¹, 夏菲^{1,2}, 陈正乐⁴, 李文丽³, 刘军港⁵,
孙岳¹, 严杰¹, 祁家明⁶

WANG Haiyang^{1,2,3}, ZHONG Fujun^{1,2}, PAN Jiayong¹, XIA Fei^{1,2}, CHEN Zhengle⁴, LI Wenli³, LIU Jungang⁵,
SUN Yue¹, YAN Jie¹, QI Jiaming⁶

1. 东华理工大学核资源与环境国家重点实验室，江西南昌 330013；
2. 中国地质学会华东放射性矿产勘查技术创新基地，江西南昌 330013；
3. 江西应用科技学院宝石矿物资源学院，江西南昌 330100；
4. 中国地质科学院地质力学研究所，北京 100081；
5. 核工业北京地质研究院，北京 100029；
6. 核工业二九〇研究所，广东韶关 512026

1. *State Key Laboratory of Nuclear Resources and Environment, East China University of Technology, Nanchang 330013, Jiangxi, China;*
2. *Innovation Base for Radiometric Mineral Exploration Technology of East China, Geological Society of China, Nanchang 330013, Jiangxi, China;*
3. *Jiangxi University of Applied Science, Gem Mineral Resources College, Nanchang 330100, Jiangxi, China;*
4. *Institute of Geomechanics, Chinese Academy of Geological Sciences, Beijing 100081, China;*
5. *Beijing Research Institute of Uranium Geology, CNCC, Beijing 100029, China;*
6. *No. 290 Research Institute, CNCC, Shaoguan 512026, Guangdong, China*

Genesis of the gneissic biotite granite in Lanhe, northern Guangdong: Constraints from zircon U-Pb geochronology, Hf isotopes, and geochemistry

Abstract: [Objective] The Lanhe pluton in northern Guangdong is located at the southeastern margin of the Zhuguangshan Complex and is primarily composed of gneissic biotite granite; its petrogenesis has not yet been determined. [Methods] This study applied LA-ICP-MS zircon U-Pb geochronology, whole-rock geochemistry, and zircon Hf isotope analyses to the Lanhe gneissic biotite granite. [Results] U-Pb dating indicates that the emplacement age of the Lanhe gneissic biotite granite is 427 ± 2 Ma, representing a product of the Caledonian magmatic activity. The geochemical characteristics show that the granite has SiO₂ contents ranging from 71.53% to 75.41%, high total alkali contents (K₂O + Na₂O = 7.57%–8.23%), and high A/CNK values (1.00–1.06). It is enriched in Rb, Th, U, and K, but depleted in Ba, Y, Nb, Ta, Sr, and Yb. The LREE/HREE ratios range from 9.49 to 28.15, with significant Eu negative anomalies ($\delta\text{Eu} = 0.21\text{--}0.76$). The zircon $\varepsilon_{\text{Hf}}(t)$ values of the samples are all negative (–11.8 to –5.2), with corresponding t_{DM2} values of 1806–2129 Ma. [Conclusion] Based on the geochemical and isotopic characteristics, the Lanhe gneissic biotite granite is

基金项目：国家自然科学基金项目（42362011，42272090）

This research is financially supported by the National Natural Science Foundation of China (Grant Nos. 42362011 and 42272090)

第一作者：王海洋（1999—），男，在读硕士，主要从事铀矿地质研究。Email: a2623716829@163.com

通信作者：潘家永（1967—），男，教授，主要从事铀矿地质教学与研究。Email: jypan@ecut.edu.cn

收稿日期：2024-12-16；修回日期：2025-02-28；录用日期：2025-03-03；网络出版日期：2025-03-04；责任编辑：吴芳

identified as a highly fractionated I-type granite, primarily formed by partial melting of crustal metasedimentary rocks, including metagraywacke and metapelite. It is likely a product of the multi-stage reworking of the Paleoproterozoic basement during the Neoproterozoic to Early Paleozoic. The comprehensive study suggests that the Lanhe gneissic biotite granite formed in a syn-collisional tectonic setting during the Early Paleozoic in South China. [Significance] Integrated with the Zhuguang magmatic system and regional geological data, the Lanhe pluton likely represents a product of the transition from compressional thickening to post-collisional extension during the Caledonian Orogeny in South China. This transition may have been associated with intracontinental tectonic reorganization or external subduction-collision processes.

Keywords: Lanhe pluton; zircon U–Pb Dating; geochemistry; granite; tectonic environment

摘要: 粤北澜河岩体位于诸广山岩体东南缘, 主要岩石类型为片麻状黑云母花岗岩, 其岩石成因尚未厘定。因此, 对澜河片麻状黑云母花岗岩开展了 LA-ICP-MS 锆石 U-Pb 年代学、岩石地球化学和锆石 Hf 同位素研究。U-Pb 定年结果显示澜河片麻状黑云母花岗岩的侵位年龄为 427 ± 2 Ma, 为加里东期岩浆活动的产物。岩石地球化学特征显示其 SiO_2 含量为 71.53%~75.41%, 具有较高的全碱含量 ($\text{K}_2\text{O} + \text{Na}_2\text{O} = 7.57\% \sim 8.23\%$) 和 A/CNK 值 (1.00~1.06), 富集 Rb、Th、U、K, 亏损 Ba、Y、Nb、Ta、Sr、Yb 等元素, LREE/HREE 为 9.49~28.15, Eu 负异常明显 ($\delta\text{Eu} = 0.21 \sim 0.76$)。样品的锆石 $\epsilon_{\text{Hf}}(t)$ 均为负值 ($-11.8 \sim -5.2$), 对应二阶段 Hf 模式年龄 (t_{DM2}) 值为 2129~1806 Ma。该结果表明澜河片麻状黑云母花岗岩为高分异 I 型花岗岩, 主要由地壳变质砂岩和变质泥岩部分熔融形成, 可能是古元古代基底在新元古代—早古生代多期改造后的产物。综合研究认为澜河片麻状黑云母花岗岩形成于华南早古生代的同碰撞构造环境。结合区域地质资料, 澜河岩体可能是华南加里东期造山运动从挤压增厚向后碰撞伸展的转变的产物, 这一转变可能与华南内部的构造重组或外部板块的俯冲碰撞有关。

关键词: 澜河岩体; 锆石 U-Pb 定年; 地球化学; 花岗岩; 构造环境

中图分类号: P54; P58 **文献标识码:** A **文章编号:** 1006-6616(2025)03-0539-18

DOI: 10.12090/j.issn.1006-6616.2024137

0 引言

华南为华夏地块和扬子地块在新元古代由江南造山带拼接而成 (Wang et al., 2013; Wang et al., 2014; Li et al., 2014; Cawood et al., 2018), 在板块运动、陆内造山等多期复合构造机制影响下, 形成了不同时期、不同规模的花岗岩 (Charvet et al., 2010; 张芳荣, 2011; 邓平等, 2011, 2012; 黄国龙等, 2012; 王丽丽, 2015; Zhang et al., 2018)。花岗质岩作为大陆上地壳的主要组成部分, 存在多种成因类型 (Chappell and White, 1974, 2001; Coleman and Peterman, 1975; Loiselle and Wones, 1979), 其不同成因类型的花岗岩及其岩石组合受大陆地壳的动力学演化过程控制。因此, 花岗岩可为地壳形成、壳幔相互作用、动力学背景和岩石圈演化等提供重要信息。华南加里东期花岗岩主要分布于安化-罗城断裂带和政和-大埔断裂带之间的闽、赣、粤、湘、桂 5 省交界地区, 从东到西、由北往南划分为武夷、武功山、南岭、桂北-桂东北、大瑶山和云开 6 个地区 (郭春

丽和刘泽坤, 2021), 主要为过铝质 S 型花岗岩, 岩浆主要来源于地壳物质的部分熔融 (李献华, 1993; 舒良树, 2006; 张芳荣等, 2009; 华仁民等, 2013; Shu et al., 2015; 舒良树等, 2020)。此外, 少量的 I 型花岗岩分布在越城岭、苗尔山、板衫铺、台山、宏夏桥和桂东等地区 (Zhang et al., 2012, 2015; Huang et al., 2013; Guan et al., 2014)。部分 I 型花岗岩中还赋存镁铁质微粒包体, 地球化学数据揭示其可能源自中-新元古代基底镁铁质岩体的熔融分异过程。 (Guan et al., 2014; Zhong et al., 2016; 刘明辉等, 2021)。近年来, 也有少量 A 型花岗岩在云开、鹅婆、西芹、付坊和营上等地陆续被发现 (彭松柏等, 2006; Feng et al., 2014; Cai et al., 2017; Qiu et al., 2018; Xin et al., 2020)。与印支期和燕山期花岗岩相比, 华南加里东期花岗岩由于受到中生代构造运动的叠加和改造作用 (Wang et al., 2013; Kong et al., 2018), 研究相对薄弱, 在一定程度上影响了对华南加里东期构造演化的研究, 关于华南加里东期花岗岩构造动力学背景和性质至今仍是 1 个颇具争议的话题 (Shu et al., 2006, 2011; Wang et al., 2013; 彭松柏等, 2016a,

2016b; Liu et al., 2018)。因此,为了更好地了解华南加里东期岩体成因及其构造背景,需要在更广泛的地区开展研究。

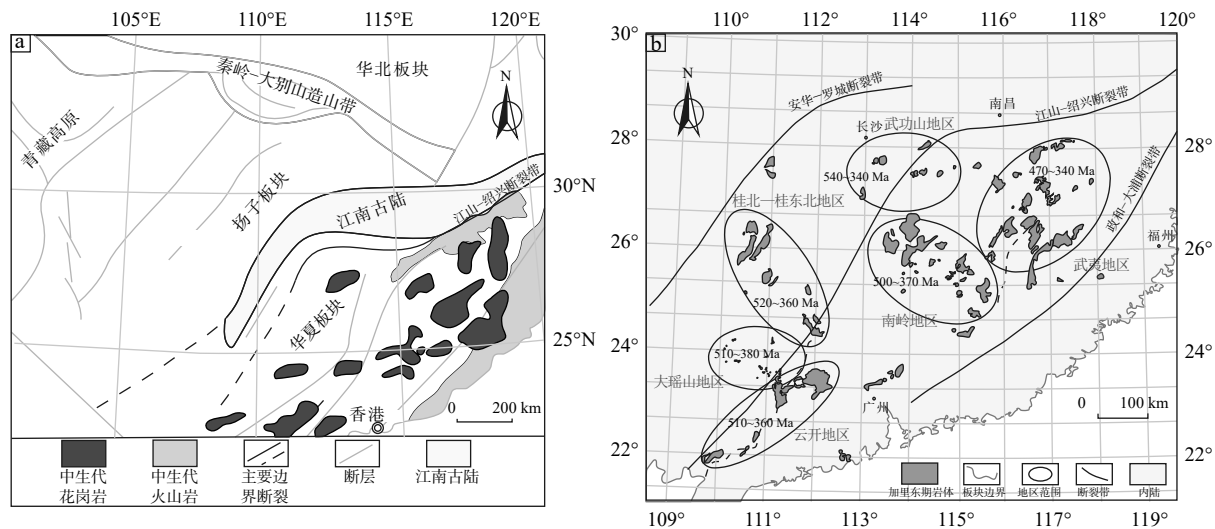
粤北诸广山岩体是中国花岗岩型铀矿床的主要产区,目前学者们主要对产出铀矿化的印支期和燕山期花岗岩开展了系统的成岩年代学、岩石成因和成矿潜力研究(Hu et al., 2008; 朱捌, 2010; 黄国龙等, 2012, 2014; 胡瑞忠等, 2019; Zhang et al., 2021; 陈柏林等, 2024; 陈柏林和裴英茹, 2025)。研究表明诸广印支期花岗岩具有高硅、高钾及低铁镁等特征,岩浆物质主要由中下地壳物质熔融形成(张素梅, 2023; 李芙蓉等, 2025);燕山期花岗岩多为S型花岗岩,主要由壳源泥质岩和杂砂岩部分熔融形成(黄国龙等, 2012, 2014; 张素梅, 2023);但关于加里东期岩浆岩的研究却鲜有报道,影响了对南岭构造的整体认识。诸广山岩体内加里东期岩浆岩主要由扶溪岩体和澜河岩体组成,而澜河岩体的岩石成因及成岩时代尚不清楚。

因此,文章以粤北诸广山岩体为研究区,选择澜河岩体片麻状黑云母花岗岩首次开展锆石 U-

Pb 年代学、全岩元素地球化学和锆石 Hf 同位素综合研究,探讨其岩石成因及构造背景,完善诸广岩浆活动谱系。

1 区域地质背景

华南东临太平洋,南部至南海,北接秦岭-大别-苏鲁高压超高压变质带构成的碰撞造山体系,西南侧通过红河走滑断裂带与印支地块实现构造拼贴(图 1a; Li et al., 2009, 2014; Xia et al., 2018)。其中华夏地块主要由南岭-云开地体和武夷地体组成,主要岩性组合包括片岩、片麻岩、斜长角闪岩、混合岩和火山碎屑岩(Yu et al., 2010)。华南在显生宙经历了早古生代造山、三叠纪印支造山、侏罗纪-白垩纪古太平洋俯冲、新生代喜马拉雅造山等多阶段的造山运动,形成大规模、强烈的岩浆活动,产出大量花岗岩(Wang et al., 2013; Kong et al., 2018),其中加里东期花岗岩的出露面积约 2200 km²(图 1b; 孙涛, 2006; 郭春丽和刘泽坤, 2021; 刘远栋等, 2022)。



a—华南区域地质构造图(据胡瑞忠等, 2004 修改); b—华南地区加里东期花岗岩分布图(据孙涛, 2006; 郭春丽和刘泽坤, 2021 修改)

图 1 华南区域地质构造与加里东期花岗岩分布图

Fig. 1 Composite map showing geological structures and granite distribution in South China

(a) Tectonic framework of South China (modified after Hu et al., 2004); (b) Distribution of Caledonian granites in South China (modified after Sun, 2006; Guo and Liu, 2021)

研究区诸广山岩体为 1 个多期多阶段复式岩体,主要岩性包括黑云母花岗岩、花岗闪长岩、辉绿岩、煌斑岩等(Hu et al., 2008; Zhang et al., 2017)。岩体呈东西向展布,主要受南岭东西向构造和诸广

山南北向构造联合控制,东侧以南雄断裂带为界,总出露面积大于 2500 km²(邓平等, 2011; 图 2)。该区的岩浆岩可划分 3 期,分别为加里东期、印支期和燕山期。加里东期岩浆岩出露面积小,由扶溪岩

体和澜河岩体组成,其中扶溪岩体岩性为花岗闪长岩(427 Ma; Zhang et al., 2018)。中生代岩浆岩是诸广山岩体主要组成部分,岩性相近,为印支—燕山构造运动背景下的产物(朱捌, 2010; 黄国龙等, 2012, 2014)。印支期岩浆岩主要分布在诸广山岩体的东部,如白云岩体、乐洞岩体等。岩体呈南北向展布,侵入体规模较大,主要由黑云母花岗岩和二云母花岗岩组成,且都为印支早期岩浆活动产物

(244~231 Ma; 邓平等, 2012; Zhang et al., 2017, 2018)。燕山期岩浆岩主要分布在诸广山岩体的南部,呈东西向展布,如三江口岩体、洪山岩体及茶山岩体等,皆为燕山早期岩浆活动的产物(162~143 Ma)。诸广山岩体基性岩脉主要形成~140 Ma、~105 Ma、~90 Ma 3个阶段,其化学成分以拉斑质玄武岩为主(李献华等, 1997; 周航兵等, 2018)。

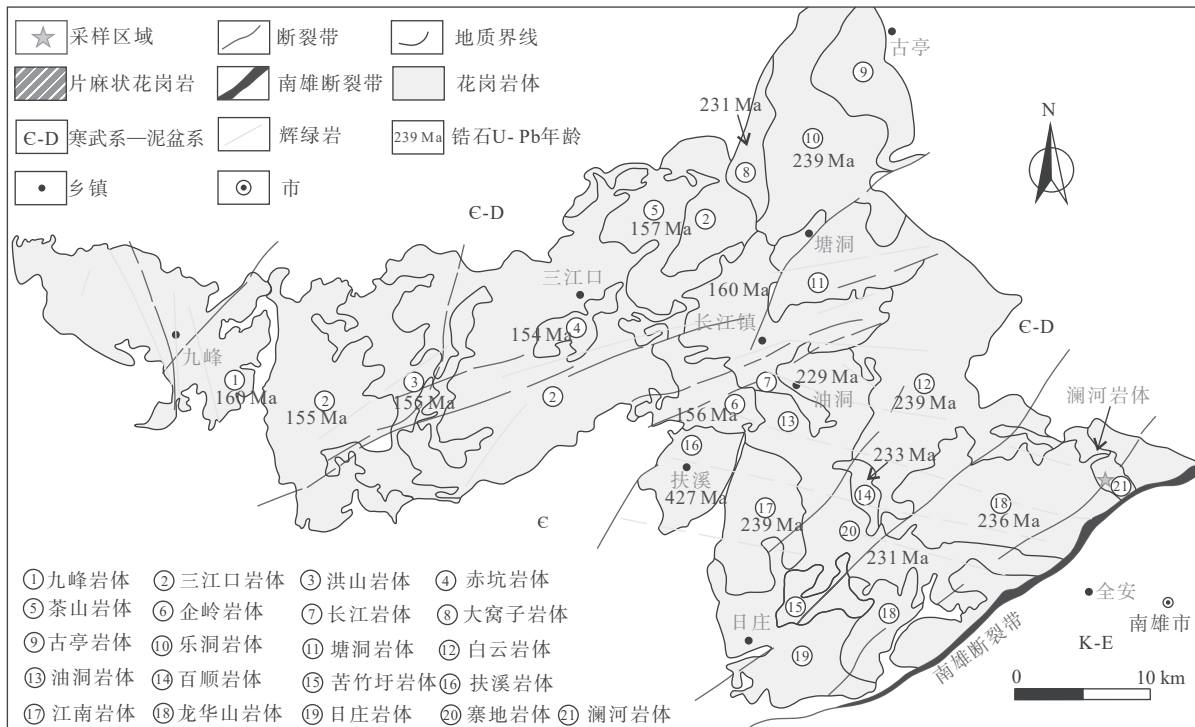


图2 粤北诸广山岩体地质简图(据邓平等, 2011修改)

Fig. 2 Geological sketch map of the Zhuguangshan Complex in northern Guangdong (modified after Deng et al., 2011)

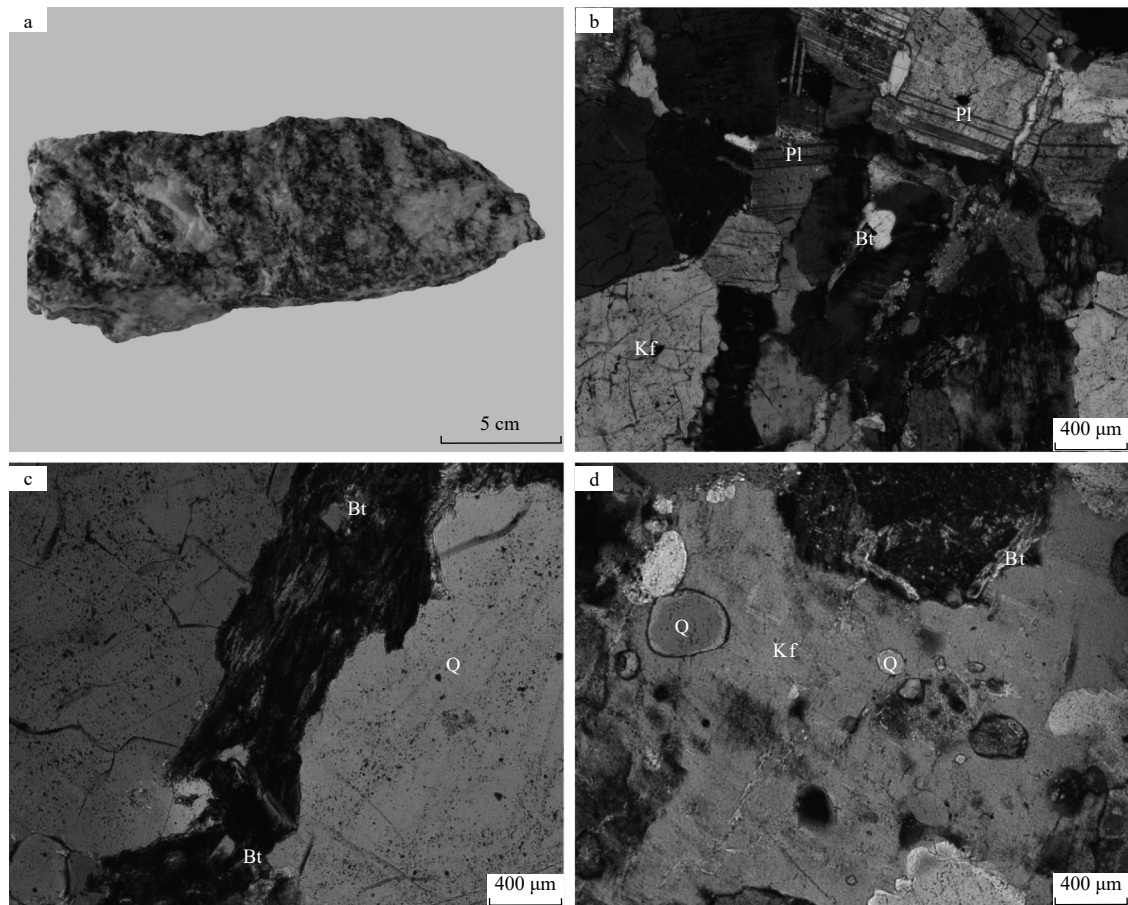
澜河岩体位于诸广山复式岩体的东南侧,面积约20 km²,受烟筒岭断裂带与牛澜断裂带构造控制,以南雄断裂带为界。澜河岩体主要岩石类型为片麻状黑云母花岗岩,岩石整体呈黑灰色,中粗粒花岗结构,片麻状构造(图3a),主要由石英(约35%)、钾长石(约25%)、斜长石(约30%)和黑云母(约5%)组成,还含有少量的锆石和磷灰石等副矿物。斜长石多呈半自形板柱状,可见聚片双晶结构,并部分发生轻微绿泥石化(图3b);黑云母呈半自形—他形片状(图3b、3c),多已绿泥石化或绿帘石化;石英多呈不规则粒状,粒径为0.2~5.0 mm(图3c);钾长石多呈半自形—他形粒状或自形斑晶,粒径在0.2~3.0 mm之间,且部分钾长石含有早期石英包裹体(图3d)。

2 实验方法

此次研究的样品均取自帽子峰镇前往南雄市公路旁采石场地表新鲜露头,坐标为114°15'25"E, 25°12'9"N。对所有样品进行主量、微量元素测试,其中样品21ZG03-1进行了LA-ICP-MS锆石U-Pb定年和Hf同位素测试。

2.1 LA-ICP-MS 锆石 U-Pb 定年

岩石经破碎、筛分、淘洗、分离等方法后分选出富锆石颗粒的重砂,然后在双目显微镜下手工精心挑选具有代表性的锆石进行年代学研究。首先将锆石颗粒粘在双面胶上,按规范流程封装在直径2.5 cm的环氧树脂靶中,待树脂充分固化后,对靶样



Kf—钾长石; Q—石英; Bt—黑云母; Pl—斜长石

a—一片麻状黑云母花岗岩手标本照片; b—一片麻状黑云母花岗岩主要矿物特征; c—一片麻状黑云母花岗岩镜下黑云母绿泥石化; d—一片麻状黑云母花岗岩镜下钾长石中的早期石英包裹体

图3 澜河片麻状黑云母花岗岩手标本及镜下照片

Fig. 3 Hand specimen and microscopic photographs of the Lanhe gneissic biotite granite

(a) Photo of gneissic biotite granite hand specimen; (b) Main mineral characteristics of gneissic biotite granite; (c) Chloritization of biotite in the gneissic biotite granite; (d) Early quartz inclusions in gneissic biotite granite under the microscope

Kf—K-feldspar; Q—quartz; Bt—biotite; Pl—plagioclase

进行逐级抛光处理光, 直至锆石颗粒内部结构清晰显露。最后采集反射光(RL)显微图像、透射光(TL)显微图像和阴极发光(CL)图像, 为 LA-ICP-MS 微区分析提供精确的靶点定位依据。其中锆石制靶委托广州拓岩检测技术有限公司完成, 阴极发光图像在东华理工大学核资源与环境国家重点实验室拍摄, 使用 NNS450 扫描电镜获取高分辨率 CL 图像。

研究采用高精度激光剥蚀电感耦合等离子体质谱(LA-ICP-MS)技术开展锆石 U-Pb 同位素定年分析, 实验在东华理工大学核资源与环境国家重点实验室完成。分析系统由 GeoLasHD 193 nm 准分子激光剥蚀系统与 Agilent 7900 四极杆质谱仪联机构成, 配备双气体(He-Ar)在线混合进样系统和信号

平滑装置。实验参数经系统优化: 激光束斑直径 32 μm , 重复频率 5 Hz, 能量密度 3.5 J/cm², 单点分析包括 20 s 背景采集和 45 s 样品信号采集。质量控制体系采用多级标样校正方案: 以国际标准锆石 91500(Wiedenbeck et al., 1995)进行 U-Pb 同位素分馏校正, Plešovice 锆石(Sláma et al., 2008)作为过程监控样, NIST SRM 610 用于微量元素分馏校正。数据处理采用 ICPMSDataCal 11.0 软件完成信号选择、背景扣除、漂移校正及同位素比值计算等步骤。最终年龄计算与谐和图绘制使用 Isoplot/Ex_ver3(Ludwig, 2003)完成, 采用 ²⁰⁶Pb/²³⁸U-²⁰⁷Pb/²³⁵U 双衰变系一致性检验, 确保年龄数据的可靠性。澜河片麻状黑云母花岗岩 LA-ICP-MS 锆石 U-Pb 年龄分析结果见表 1。

表 1 澜河岩体 LA-ICP-MS 锆石 U-Pb 同位素定年分析结果

Table 1 LA-ICP-MS zircon U-Pb isotopic data of the Lanhe pluton

测点号	U Th Pb			$^{207}\text{Pb}/^{206}\text{Pb}$		$^{207}\text{Pb}/^{235}\text{U}$		$^{206}\text{Pb}/^{238}\text{U}$		$^{207}\text{Pb}/^{235}\text{U}$		$^{206}\text{Pb}/^{238}\text{U}$	
	/($\times 10^{-6}$)			同位素比值	2σ	同位素比值	2σ	同位素比值	2σ	年龄/Ma	2σ	年龄/Ma	2σ
21ZG03-1-1	274	72	22	0.0581	0.0037	0.5479	0.0349	0.0684	0.0016	444	23	426	9
21ZG03-1-2	419	47	32	0.0541	0.0032	0.5128	0.0349	0.0686	0.0020	420	23	428	12
21ZG03-1-3	534	56	40	0.0549	0.0033	0.5301	0.0354	0.0688	0.0026	432	23	429	16
21ZG03-1-4	654	36	49	0.0535	0.0026	0.5048	0.0256	0.0684	0.0014	415	17	427	8
21ZG03-1-5	488	57	37	0.0537	0.0035	0.4952	0.0304	0.0673	0.0016	408	21	420	9
21ZG03-1-6	208	55	16	0.0500	0.0036	0.4733	0.0368	0.0688	0.0023	393	25	429	14
21ZG03-1-7	785	52	59	0.0522	0.0023	0.4957	0.0234	0.0687	0.0014	409	16	429	9
21ZG03-1-8	547	69	42	0.0546	0.0028	0.5105	0.0280	0.0676	0.0013	419	19	422	8
21ZG03-1-9	485	70	37	0.0537	0.0028	0.4975	0.0264	0.0673	0.0017	410	18	420	10
21ZG03-1-10	923	88	69	0.0531	0.0026	0.5053	0.0262	0.0690	0.0018	415	18	430	11
21ZG03-1-11	1401	120	107	0.0527	0.0023	0.4952	0.0218	0.0681	0.0012	408	15	425	7
21ZG03-1-12	961	269	77	0.0543	0.0026	0.5137	0.0255	0.0686	0.0017	421	17	428	10
21ZG03-1-13	448	60	34	0.0541	0.0034	0.5035	0.0312	0.0676	0.0017	414	21	422	10
21ZG03-1-14	754	60	57	0.0519	0.0027	0.4906	0.0270	0.0685	0.0017	405	18	427	10
21ZG03-1-15	519	66	39	0.0514	0.0027	0.4778	0.0249	0.0675	0.0016	397	17	421	10
21ZG03-1-16	654	751	62	0.0539	0.0025	0.5082	0.0266	0.0682	0.0018	417	18	425	11
21ZG03-1-17	1194	77	90	0.0531	0.0021	0.5070	0.0242	0.0690	0.0018	416	16	430	11
21ZG03-1-18	765	58	60	0.0540	0.0023	0.5299	0.0249	0.0710	0.0016	432	17	442	10
21ZG03-1-19	582	54	47	0.0572	0.0026	0.5538	0.0274	0.0701	0.0018	448	18	437	11
21ZG03-1-20	367	57	29	0.0550	0.0033	0.5168	0.0315	0.0680	0.0014	423	21	424	9
21ZG03-1-21	727	90	57	0.0542	0.0024	0.5176	0.0248	0.0691	0.0014	424	17	430	8
21ZG03-1-22	790	43	59	0.0529	0.0028	0.5141	0.0276	0.0706	0.0019	421	18	440	12
21ZG03-1-23	576	97	46	0.0550	0.0026	0.5156	0.0248	0.0679	0.0011	422	17	424	7
21ZG03-1-24	1148	124	88	0.0543	0.0021	0.5152	0.0225	0.0688	0.0018	422	15	429	11
21ZG03-1-25	906	86	69	0.0551	0.0023	0.5231	0.0247	0.0687	0.0018	427	16	429	11
21ZG03-1-26	399	44	30	0.0570	0.0031	0.5457	0.0339	0.0692	0.0019	442	22	431	12
21ZG03-1-27	749	63	58	0.0545	0.0027	0.5149	0.0254	0.0686	0.0012	422	17	428	7

2.2 锆石 Lu-Hf 同位素分析

锆石 Hf 同位素的测试分析工作在南京聚谱检测科技有限公司完成。选择已经做过锆石年龄的锆石,在相应的阴极发光图像特征的位置上使用仪器型号为 Nu Plasma II 的多接收器型号电感耦合等离子体质谱仪 (MC-ICP-MS) 进行测试,进样系统为 193 nm ArF 准分子激光剥蚀系统 (Resonetics)。仪器激光束直径为 40 μm , 能量密度为 3.5 J/cm^2 , 剥蚀频率为 8 Hz, 每个点位剥蚀 40 s。在分析样品的同时测试锆石国际标样 GJ-1、91500 和 Plešovice, 以监测仪器状态和数据漂移程度, 确保锆石 Hf 同位素比值数据质量。 ϵ_{Hf} 计算采用 ^{176}Lu 衰变常数为 $1.867 \times 10^{-11} \text{y}^{-1}$ (Söderlund, 2004), 球粒陨石现今值 $^{176}\text{Lu}/^{177}\text{Hf}=$

0.282785 和 $^{176}\text{Lu}/^{177}\text{Hf}=0.0336$ (Bouvier et al., 2008)。亏损地幔 Hf 模式年龄 (t_{DM}) 以现今亏损值 $^{176}\text{Lu}/^{177}\text{Hf}=0.28325$ 、 $^{176}\text{Lu}/^{177}\text{Hf}=0.0384$ 计算, 二阶段 Hf 模式年龄 (t_{DM2}) 计算采用上地壳平均值 $^{176}\text{Lu}/^{177}\text{Hf}=0.015$ (Griffin et al., 2002)。

2.3 全岩地球化学分析

采用标准化岩石样品制备与分析流程: 野外采集的新鲜样品经初步破碎后, 严格去除风化蚀变部分, 经去离子水超声清洗并烘干后, 使用颚式破碎机将样品破碎至 <5 mm 粒径, 最后采用玛瑙研钵研磨至 200 目 (<74 μm) 以下, 确保样品均匀性和代表性。所有样品制备与分析测试均在武汉上谱分析科技有限责任公司完成。主量元素分析采用 ZSX

Primus II 型波长色散 X 射线荧光光谱仪 (XRF) 测定, 仪器工作参数为: X 射线管电压 50 kV, 电流 60 mA。烧失量 (LOI) 通过重量法在 1000°C 条件下测定。采用理论 α 系数法进行基体效应校正, 主量元素分析精度优于 1%, 相对标准偏差 (RSD) 控制在 2% 以内。微量元素分析使用 Agilent 7700e 型电感耦合等离子体质谱仪 (ICP-MS) 完成。样品经氢氟酸-硝酸高压消解罐消解后, 采用 Rh 内标法进行仪器漂移校正, 分析精度优于 10%。全过程采用国家一级标准物质 (GBW 系列) 进行质量监控, 确保数据准确性和可靠性。

3 分析结果

3.1 U-Pb 定年

从 CL 图像可以看出, 澜河片麻状黑云母花岗岩样品 (21ZG03-1) 锆石颗粒晶形完好, 呈长柱状或等轴状, 长轴粒径约 90~200 μm , 长宽比在 1:1 到

2:1 之间, 大部分锆石具有明显的振荡环带 (图 4)。测点均选择在韵律环带结构发育的位置, 少数选择在边部环带结构较清晰的位置。澜河片麻状黑云母花岗岩 LA-ICP-MS 锆石 U-Pb 年龄分析结果显示 (附表 1), 样品中锆石的 Th、U 含量分别为 $43.3 \times 10^{-6} \sim 269 \times 10^{-6}$ 、 $208 \times 10^{-6} \sim 1401 \times 10^{-6}$, Th/U 的比值为 0.05~0.28, 平均值为 0.16, 大于 0.1, 具有岩浆锆石特征 (Wu and Zheng, 2004)。该样品共测试 27 个分析点, 数据投影点均落于谐和线或其附近, 谐和度均大于 90%, $^{206}\text{Pb}/\text{U}^{238}$ 年龄变化为 420~442 Ma, 加权平均年龄为 427 ± 2 Ma (MSWD=1.17, $n=27$; 图 5), 该年龄代表了岩体的结晶年龄。

3.2 元素地球化学

3.2.1 主量元素特征

澜河片麻状黑云母花岗岩的主量元素含量见表 2。岩石的烧失量 (LOI) 值为 0.52%~1.39%, 表明经历的风化或蚀变程度低。分析结果显示, 样品具有较高的 SiO_2 (71.53%~75.41%) 和 Al_2O_3 含量 (11.93%~

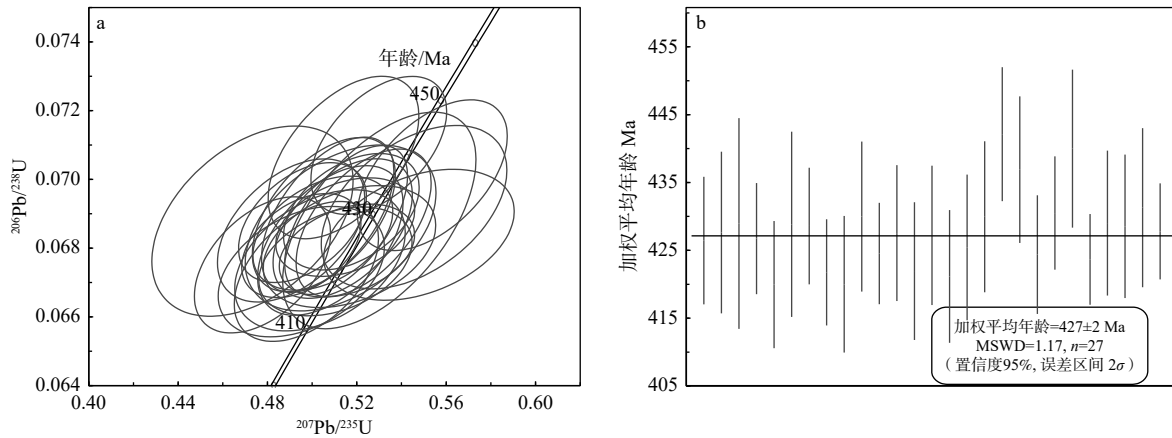


白色圈代表 U-Pb 年龄测试点, 灰色圈代表 Hf 同位素测试点

图 4 澜河片麻状黑云母花岗岩锆石 CL 图像

Fig. 4 CL images of zircon from the gneissic biotite granite of the Lanhe pluton

The white circles represent U-Pb age analysis points, and the gray circles represent Hf isotope analysis points



a—澜河片麻状黑云母花岗岩锆石年龄谐和图；b—澜河片麻状黑云母花岗岩锆石年龄加权图

图5 澜河片麻状黑云母花岗岩锆石谐和年龄及加权平均图

Fig. 5 U-Pb zircon geochronology for the gneissic biotite granite from the Lanhe pluton

(a) U-Pb concordia diagram of zircon of the Lanhe gneissic biotite granite; (b) Weighted mean zircon age of the Lanhe gneissic biotite granite

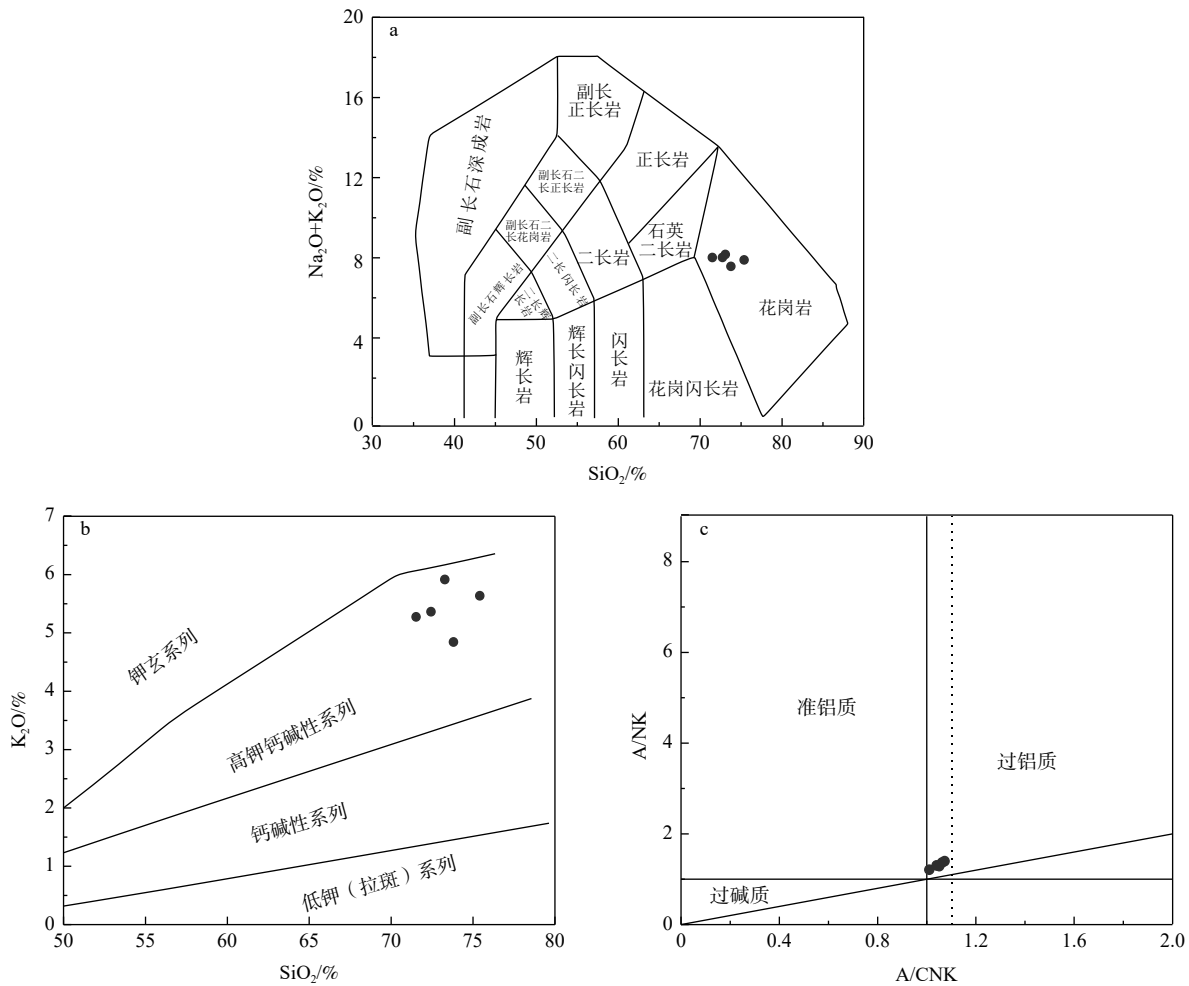
表2 澜河岩体主量(%)和微量元素($\times 10^{-6}$)组成

Table 2 Major (%) and trace element ($\times 10^{-6}$) contents of the granites of the Lanhe pluton

岩性	黑云母花岗岩										
样品编号	21ZG03-1	21ZG03-2	21ZG03-3	21ZG03-4	21ZG03-5	样品编号	21ZG03-1	21ZG03-2	21ZG03-3	21ZG03-4	21ZG03-5
SiO ₂	73.81	71.53	75.41	72.43	73.28	Pr	11.38	15.54	4.93	12.42	10.69
TiO ₂	0.28	0.40	0.20	0.32	0.28	Sr	86.49	78.10	75.91	55.22	117.78
Al ₂ O ₃	13.68	14.04	11.93	13.17	13.39	Nd	44.08	58.15	18.15	45.65	37.68
TFe ₂ O ₃	2.21	3.10	1.57	2.25	1.80	Zr	145.20	177.07	61.26	158.05	153.42
MnO	0.02	0.03	0.02	0.06	0.02	Hf	4.71	5.57	2.07	5.17	5.10
MgO	0.50	0.69	0.36	0.50	0.45	Sm	8.59	11.63	3.81	11.31	5.86
CaO	1.71	1.70	1.15	1.34	1.51	Eu	0.82	0.84	0.80	0.80	1.24
Na ₂ O	2.73	2.74	2.25	2.65	2.32	Y	8.31	10.28	7.57	23.87	6.09
K ₂ O	4.85	5.27	5.64	5.36	5.92	Yb	0.45	0.58	0.50	1.42	0.44
P ₂ O ₅	0.04	0.04	0.04	0.05	0.05	Lu	0.07	0.08	0.07	0.23	0.07
LOI	0.59	0.57	1.02	1.39	0.55	Gd	6.44	8.73	3.29	10.99	3.64
SUM	100.41	100.10	99.58	99.52	99.53	Tb	0.66	0.87	0.37	1.40	0.37
Na ₂ O+K ₂ O	7.57	8.01	7.89	8.02	8.23	Dy	2.55	3.05	1.77	5.95	1.51
K ₂ O/Na ₂ O	1.78	1.93	2.51	2.02	2.55	Ho	0.33	0.43	0.28	0.87	0.23
A/NK	1.40	1.37	1.21	1.29	1.31	Er	0.65	0.83	0.66	1.95	0.54
A/CNK	1.06	1.05	1.00	1.04	1.03	Tm	0.07	0.09	0.08	0.23	0.07
CaO/Na ₂ O	0.63	0.62	0.51	0.51	0.65	ΣREE	219.93	292.45	95.01	241.80	200.34
Al ₂ O ₃ /TiO ₂	48.68	34.83	59.96	41.80	47.47	LREE	208.71	277.79	87.99	218.76	193.47
Rb	186.46	238.32	205.64	208.07	224.03	HREE	11.22	14.66	7.02	23.04	6.87
Ba	489.10	459.74	503.00	461.83	639.68	LREE/HREE	18.60	18.94	12.53	9.49	28.15
Th	37.22	51.46	13.93	33.28	63.43	La _N /Yb _N	70.10	72.23	25.82	22.44	69.84
U	2.92	4.16	2.02	4.01	3.58	δEu	0.32	0.24	0.68	0.21	0.76
Nb	11.26	14.67	8.31	10.55	6.62	T _{Zr} /°C	758.37	771.32	695.06	767.49	762.36
Ta	0.31	0.44	0.21	0.29	0.21						
La	46.72	61.61	19.17	46.85	45.14						
Ce	97.11	130.02	41.12	101.73	92.87						

14.04%); 较高的碱含量, Na₂O 含量为 2.25%~2.74%, K₂O 含量为 4.85%~5.92%, 全碱 (K₂O+Na₂O) 含量介于 7.57%~8.23% 之间。在岩石 TAS 图解中, 样品均落入花岗岩区域内(图 6a)。样品相对富钾, K₂O/Na₂O 值为 1.78~2.55, 平均为 2.16, 在 SiO₂-K₂O 图解

中, 样品均落入高钾钙碱性系列区域内(图 6b)。铝饱和指数 (A/CNK) 值为 1.00~1.06, 平均为 1.04, 显示弱过铝质特征, 在 A/CNK-A/NK 图解中, 均落入过铝质区域内(图 6c)。



a—TAS 图解 (Middlemost, 1994); b—SiO₂-K₂O 图解 (Peccerillo and Taylor, 1976); c—A/CNK-A/NK 图解 (Maniar and Piccoli, 1989)

图 6 澜河片麻状黑云母花岗岩 TAS、SiO₂-K₂O 与 A/CNK-A/NK 图解

Fig. 6 TAS, SiO₂-K₂O and A/CNK-A/NK diagrams of the gneissic biotite granite from the Lanhe pluton

(a) TAS diagram (Middlemost, 1994); (b) SiO₂ vs. K₂O diagram (Peccerillo and Taylor, 1976); (c) A/CNK vs. A/NK diagram (Maniar and Piccoli, 1989)

3.2.2 微量元素与稀土元素特征

澜河片麻状黑云母花岗岩微量元素含量见表 2。在原始地幔标准化微量元素蛛网图中(图 7a), 澜河片麻状黑云母花岗岩相对富集 Rb、Th、U, 相对亏损 Ba、Nb、Ta、Sr、Zr、Hf。黑云母花岗岩具有较高的稀土总量 (ΣREE=95.01×10⁻⁶~200.34×10⁻⁶), Eu 负异常明显 (δEu=0.21~0.76)。在球粒陨石标准化稀土配分图解中(图 7b), 澜河片麻状黑云母花岗岩呈

右倾型, LREE/HREE 为 9.49~28.15, 平均为 17.54, (La/Yb)_N 值为 22.44~72.23, 反映轻重稀土分馏明显, 轻稀土较为富集。

3.3 锆石 Hf 同位素特征

澜河岩体片麻状黑云母花岗岩 16 颗锆石 Hf 同位素分析结果显示(详见 OSID 码中图表), 锆石 ¹⁷⁶Hf/¹⁷⁷Hf 初始值为 0.282181~0.282369, 对应的 ε_{Hf}(t) 值为 -11.8~-5.2(图 8a), 主要集中在 -5.2~-9.0 之间



a—微量元素原始地幔标准化蛛网图；b—稀土元素球粒陨石标准化图解

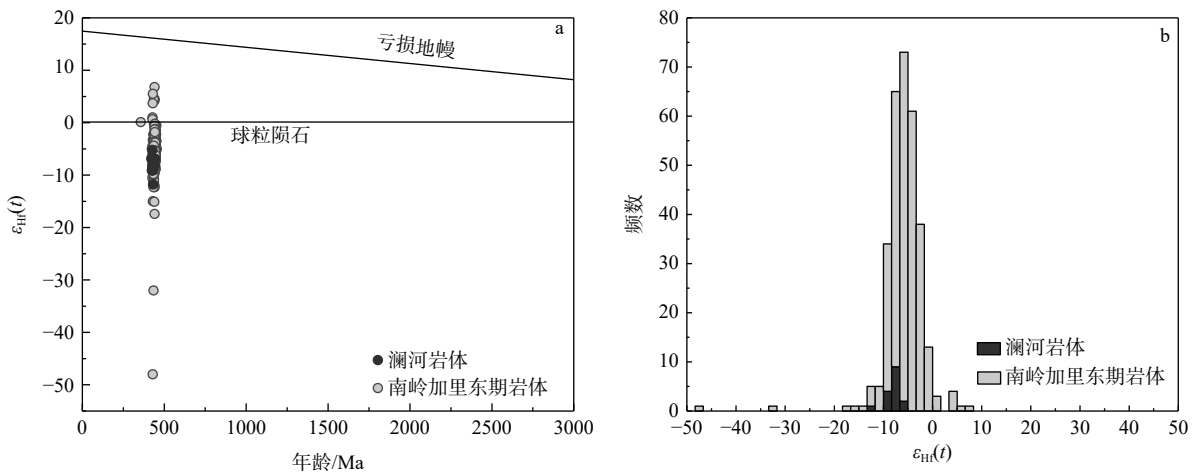
图7 澜河片麻状黑云母花岗岩微量元素和稀土元素图解（标准化数据引自 Sun and McDonough, 1989）

Fig. 7 Trace element and REE diagrams of the Lanhe gneissic biotite granite (normalization values from Sun and McDonough, 1989)

(a) Primitive mantle-normalized trace element spider diagram; (b) Chondrite-normalized rare earth element diagram

(图 8b), 二阶段 Hf 模式年龄 (t_{DM2}) 为 1806~2129 Ma, 显著大于岩体结晶年龄 (427 Ma)。Hf 模式年龄反映的是锆石源区物质从亏损地幔中分异的时间,

而非直接限定岩浆熔融事件的时代 (Griffin et al., 2002)。



a—锆石 $\epsilon_{Hf}(t)$ -年龄演化图；b— $\epsilon_{Hf}(t)$ 频数分布直方图

图8 锆石 $\epsilon_{Hf}(t)$ 演化与分布特征（其他 Hf 同位素数据引自王丽丽, 2015 和徐文景, 2017）

Fig. 8 $\epsilon_{Hf}(t)$ vs. U-Pb age plot for zircon from the granitic rock and $\epsilon_{Hf}(t)$ histogram (Other Hf isotope data are quoted from Wang, 2015 and Xu, 2017)

(a) Zircon $\epsilon_{Hf}(t)$ vs. age evolution map; (b) $\epsilon_{Hf}(t)$ frequency distribution histogram

4 讨论

4.1 华南加里东期岩浆事件

早古生代末, 扬子克拉通、华夏地块等发生板内造山运动, 导致震旦纪—早古生代海槽关闭和华南大部分地区前泥盆系变形地层及其上覆泥盆纪

地层之间发生区域性角度不整合, 形成了华南加里东造山带, 引发了强烈的岩浆作用、变质和变形作用, 形成大规模的加里东期花岗岩 (舒良树等, 2006; Charvet et al., 2010; Li et al., 2010; 张芳荣, 2011; 王丽丽, 2015; Xu and Xu, 2015; Shu et al., 2015), 其中以南岭地区加里东期岩体的数量居多。针对南岭地区加里东期岩浆岩, 研究已获取一大批高精

度定年数据(张芳荣, 2011; 王丽丽, 2015; Xu and Xu, 2015; Zhang et al., 2018), 但是其中南岭地区的澜河岩体的形成时代一直没有很好地限定。中国科学院贵阳地球化学研究所同位素年龄实验室和湖北地质科学研究所同位素年龄实验室(1972)曾对澜河片麻状黑云母花岗岩中的黑云母矿物开展 K-Ar 法定年, 初步认定澜河岩体属于印支期产物; 王联魁等(1975)利用单颗粒锆石 U-Pb 定年法测得澜河岩体成岩年龄为 372 Ma; 邓访陵(1987)综合运用单颗粒锆石 U-Pb 定年法、K-Ar 和 Rb-Sr 法判定澜河岩体形成时代为加里东期甚至更早(≥ 424 Ma)。可以看出, 应用上述传统测年方法测得澜河岩体形成年龄较分散, 难以准确限定岩体的形成时代。

近年来, 随着锆石 SHRIMP U-Pb、TIMS、激光剥蚀等离子质谱 LA-ICP-MS 等方法的发展, 花岗岩成岩年龄的精度与可靠性得到了巨大提升。此次所测岩体锆石均为岩浆锆石。在岩浆活动中, U 和 Th 元素具有相似的地球化学性质, 能够以类质同象代替的方式进入锆石晶格中(Jensen, 1973; Nardi et al., 2013)。一般情况下, 锆石中的 U 和 Th 元素具有相对稳定的配分系数, 因而在单一岩浆演化过程中, 锆石的 Th/U 比值会保持相对稳定。此次对澜河片麻状黑云母花岗岩采用高精度 LA-ICP-MS 锆石 U-Pb 法, 年龄谐和度高, Th/U 比值接近, 获得澜河岩体形成年龄为 427 ± 2 Ma (MSWD=1.17, $n=27$), 准确限定了其形成时代, 为华南加里东期岩浆活动的产物。

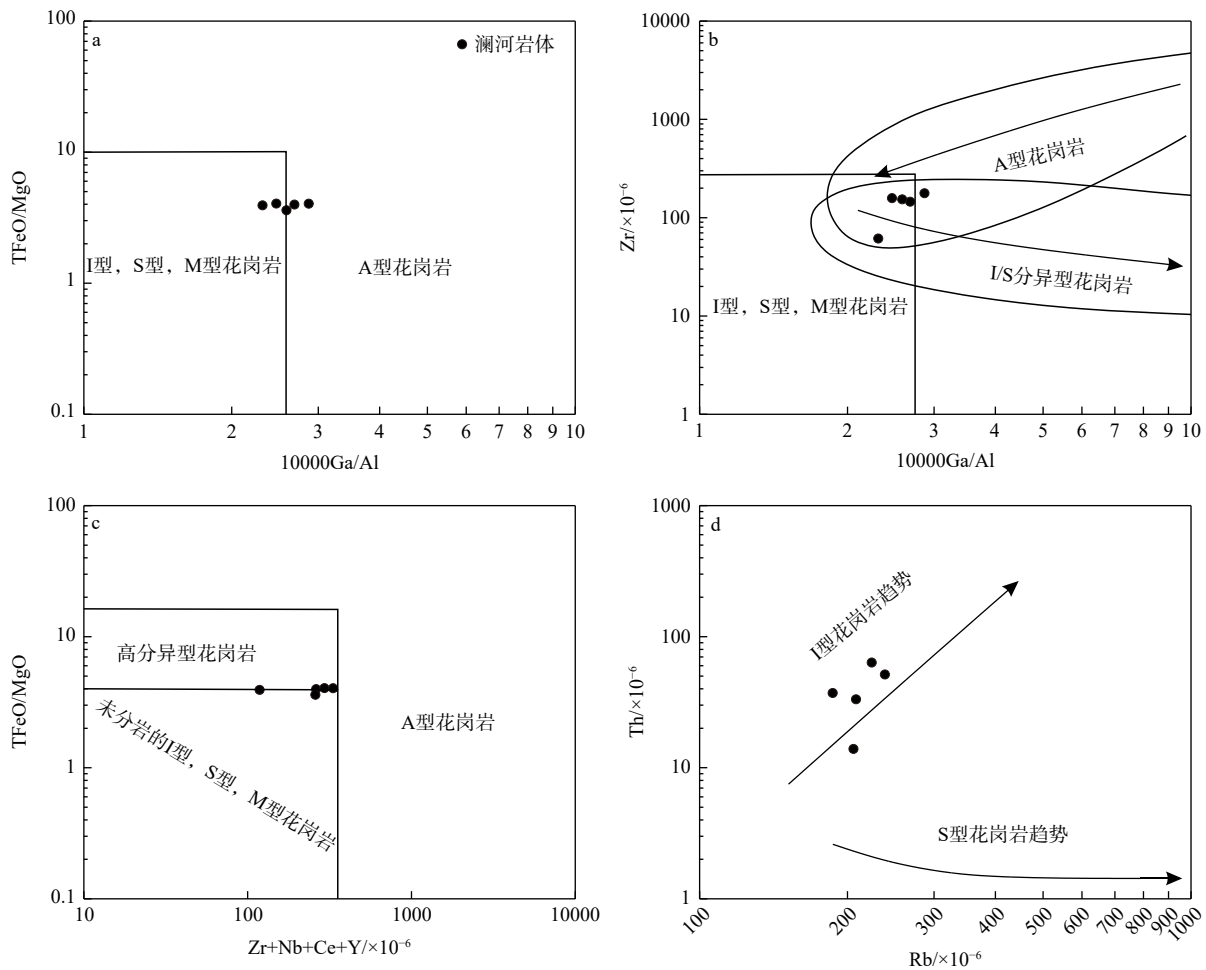
4.2 岩体的分类及成因

对花岗岩进行分类可用来判别岩石来源和成因, 一般分为 I 型、S 型、M 型和 A 型, 其中 I 型和 S 型可根据物源特征进行区分(Chappell and White, 1974; Loiselle and Wones, 1979)。A 型花岗岩中常见碱性暗色矿物, 一般很少或不含斜长石, 以及 $Zr+Nb+Ce+Y$ 值大于 350×10^{-6} (Whalen et al., 1987), 而澜河片麻状黑云母花岗岩斜长石含量高, 未见有碱性暗色矿物, 且 $Zr+Nb+Ce+Y$ 值 ($118 \times 10^{-6} \sim 332 \times 10^{-6}$) 低于 A 型花岗岩的相应值。此外, 根据 Watson and Harrison(1983) 锆饱和温度计, 计算出澜河片麻状黑云母花岗岩锆饱和温度为 $695 \sim 771$ °C, 平均为 751 °C。因此澜河片麻状黑云母花岗岩不属于 A 型花岗岩。澜河片麻状黑云母花岗岩的 $\epsilon_{\text{Hf}}(t)$ 值均为负值, 并含有少量的继承锆石, 也不可能属于 M 型花岗岩。所有样品具有高 SiO_2 (71.53%~75.41%)、

富 K_2O (4.85%~5.92%), 贫 CaO (1.15%~1.71%)、 MgO (0.36%~0.69%)、低 TFe_2O_3 (1.80%~3.10%)、 TiO_2 (0.20%~0.40%)、 P_2O_5 (0.04%~0.05%) 的特点, 表明岩石经历了高分异演化作用。在 A 型花岗岩判别图解中(图 9a—9c), 样品落入 I 与 A 型花岗岩区域, 但与吴福元等(2007)提出的高分异 I/S 型花岗岩演化趋势一致。镜下观察发现, 澜河片麻状黑云母花岗岩中没有典型的富铝矿物(像白云母、堇青石和石榴子石等)以及其他暗色碱性矿物, 暗色矿物主要为黑云母。其铝饱和指数 A/CNK 值处于 1.00~1.06 之间, 数值不高, 且 Rb 和 Th 含量呈现明显的正相关关系(图 9d), 这些都表明它并非 S 型花岗岩。综上所述, 澜河片麻状黑云母花岗岩为高分异 I 型花岗岩。

结合地球化学及同位素特征, 澜河片麻状黑云母花岗岩主要来源于地壳沉积岩的部分熔融, 证据如下: ①澜河片麻状黑云母花岗岩主量元素显示 SiO_2 含量高(71.53%~75.41%), 镁铁质成分较低; ②部分高场强元素和大离子亲石元素可以示踪岩浆岩物质来源。澜河岩体花岗岩的 Rb/Sr (1.90~3.77, 平均为 2.72) 和 Rb/Nd 比值 (16.24~33.82, 平均为 22.22) 均远远高于中国东部(分别为 0.31 和 6.8; 高山等, 1999) 和全球上地壳的平均值(分别为 0.32 和 4.5; Taylor and McLennan, 1985), 表明澜河片麻状黑云母花岗岩具有高成熟度的壳源成因的特征; ③地壳沉积岩起源的花岗岩通常富集 Th 及具有较高的 $\text{Al}_2\text{O}_3/\text{TiO}_2$ 比值(Sylvester, 1998; Plank and Langmuir, 1998), 澜河片麻状黑云母花岗岩具有较高的 Th 含量和 $\text{Al}_2\text{O}_3/\text{TiO}_2$ 比值 (13.9~63.4; 34.8~48.7), 表明其源区也主要是沉积物; ④澜河片麻状黑云母花岗岩与南岭地区加里东期花岗质岩体具有相似 Hf 同位素组成(图 8a), $\epsilon_{\text{Hf}}(t)$ 值为 -11.8~-5.2, 二阶段 Hf 模式年龄 (t_{DM2}) 为 2129~1806 Ma, 说明二者的源区相似, 均主要由地壳沉积岩部分熔融形成(Xu and Xu, 2015; 王丽丽, 2015)。⑤在 $\text{CaO}/\text{MgO}+\text{TFeO}-\text{Al}_2\text{O}_3/(\text{MgO}+\text{TFeO})$ 和 Rb/Sr-Rb/Ba 图解中(图 10), 澜河片麻状黑云母花岗岩主要分布在砂屑岩源区区域内, 少量落入泥质岩区域内, 表明澜河片麻状黑云母花岗岩起源于以变质砂岩和变质泥岩为主的源区的部分熔融。

结合区域地质背景, 华南加里东期花岗岩的源区可能经历了多阶段演化: ①古元古代 (2.1~1.8 Ga) 地壳物质从亏损地幔分异, 形成华南基底岩石



a—10000Ga/Al-TFeO/MgO 图解 (Whalen et al., 1987); b—10000Ga/Al-Zr 图解 (Whalen et al., 1987); c—Zr+Nb+Ce+Y-TFeO/MgO 图解 (吴福元等, 2007); d—Rb-Th 图解 (Whalen et al., 1987)

图9 澜河片麻状黑云母花岗岩岩石成因类型判别图解

Fig. 9 Genetic discrimination diagrams of the gneissic biotite granites of the Lanhe pluton

(a) 10000Ga/Al vs. TFeO/MgO diagram (Whalen et al., 1987); (b) 10000Ga/Al vs. Zr diagram (Whalen et al., 1987); (c) Zr+Nb+Ce+Y vs. TFeO/MgO diagram (Wu et al., 2007); (d) Rb vs. Th diagram (Whalen et al., 1987)

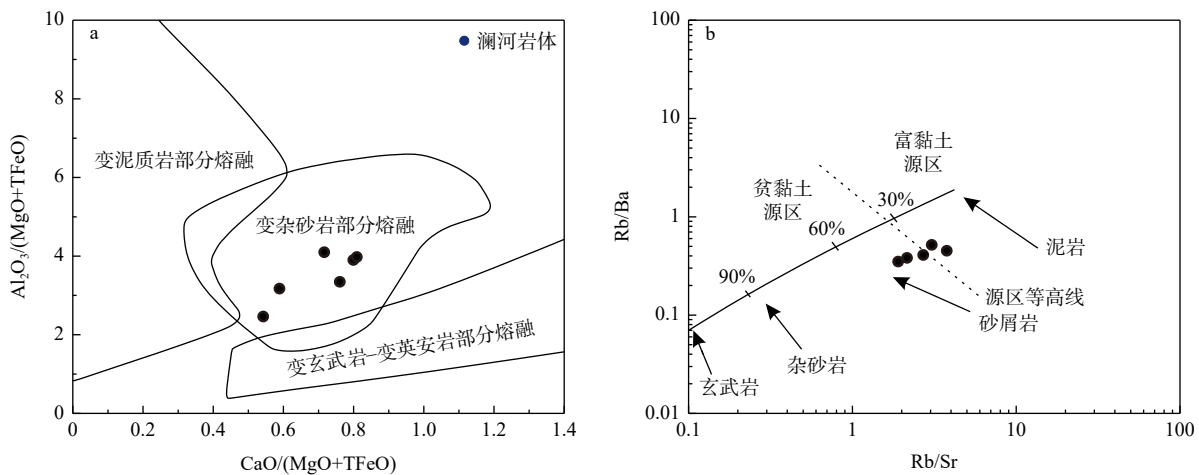
(Li et al., 2014; Xia et al., 2018); ②新元古代—早古生代, 基底岩石在加里东造山期(460~420 Ma)经历变质作用或地壳重熔 (Shu et al., 2015; 舒良树等, 2020); ③加里东晚期(~427 Ma)部分熔融形成的岩浆侵位, 形成澜河岩体。因此, 古元古代的Hf模式年龄并不代表岩体直接由古元古代地壳物质熔融形成, 而更可能指示源区物质的初始分异时间, 其后经历了多期的地壳再造过程 (Zhao et al., 2021)。

综上所述, 澜河片麻状黑云母花岗岩为高分异I型花岗岩, 主要由地壳变质砂岩和变质泥岩部分熔融形成, 可能是古元古代基底在新元古代—早古生代多期改造后的产物。

4.3 构造背景

澜河片麻状黑云母花岗岩微量元素显示较低

的Y、Nb和Yb含量, 具有火山弧花岗岩或同碰撞花岗岩的特征 (图11a)。在R1-R2 (图11b) 和Rb/30-Hf-Ta \times 3构造判别图解 (图11c) 中, 样品也基本落在同碰撞花岗岩区域附近。此外, Sr-Yb判别图解 (图11d) 显示样品均落在II区域, 对应地壳加厚的造山阶段。这些特征表明澜河岩体形成于同碰撞构造环境。研究表明, 华南加里东期花岗岩总体上分为造山挤压增厚(460~430 Ma)和后造山伸展垮塌(430~410 Ma)2个阶段, 约430~425 Ma发生了由碰撞挤压向造山后伸展的构造转换 (张芳荣等, 2009; Wang et al., 2011; 舒良树, 2012)。澜河岩体的形成年龄(427 \pm 2 Ma)恰好处于这一构造转换的关键时期, 可能是华南加里东期造山运动从挤压增厚向



a—CaO/(MgO+TFeO)—Al₂O₃/(MgO+TFeO) 图解 (Altherr et al., 2000); b—Rb/Sr—Rb/Ba 图解 (Sylvester, 1998)

图 10 澜河片麻状黑云母花岗岩源区图解

Fig. 10 Provenance diagrams of the Lanhe gneissic biotite granites

(a) CaO/(MgO+TFeO) vs. Al₂O₃/(MgO+TFeO) diagram (Altherr et al., 2000); (b) Rb/Sr vs. Rb/Ba diagram (Sylvester, 1998)

后碰撞伸展的转变的产物。

华南早古生代经历了 1 期重要的构造事件, 其属性一直是争论的焦点之一 (Charvet et al., 2010; Li et al., 2010; Shu et al., 2014, 2015, 2018; Xu et al., 2016; Lin et al., 2018; Liu et al., 2018; Wang et al., 2022, 2023, 2024)。近年来, 传统的陆内造山模型受到了挑战, 新的构造模型不断被提出。Li et al. (2022) 提出了华南早古生代可能经历了洋-陆碰撞的观点, 认为华南与东冈瓦纳大陆的俯冲碰撞可能是加里东期造山运动的主要驱动力。这个模型为解释华南缺乏典型俯冲相关岩石 (如蛇绿岩、弧火山岩) 提供了新的思路。同位素示踪体系显示, 华南加里东期花岗岩 $\varepsilon_{\text{Hf}}(t)$ 值呈现 -59.3 至 +9.53 的宽谱系分布 (郭春丽和刘泽坤, 2021), 指示既有古老地壳再造, 也有新生幔源物质加入。华南地区高压变质作用 (450~440 Ma) 与同碰撞岩浆作用 (460~430 Ma) 存在 ~20 Ma 的时间差 (Shu et al., 2015), 暗示碰撞过程具有多阶段特征。澜河片麻状黑云母花岗岩的 Hf 同位素特征和地球化学数据表明由地壳沉积岩部分熔融形成, Li et al. (2022) 提出的洋-陆碰撞模型中地壳物质部分熔融的观点一致。Wang et al. (2022, 2023, 2024) 则提出了华南内部俯冲-碰撞模式, 认为华南早古生代造山运动可能是由于华夏地块与扬子克拉通之间的斜向碰撞或走滑造山作用引起的。这一模型强调了华南内部的构造复杂性, 并认为加里东期花岗岩的形成与陆内俯冲或板内变形密切相关。澜河片麻状黑云母花岗岩

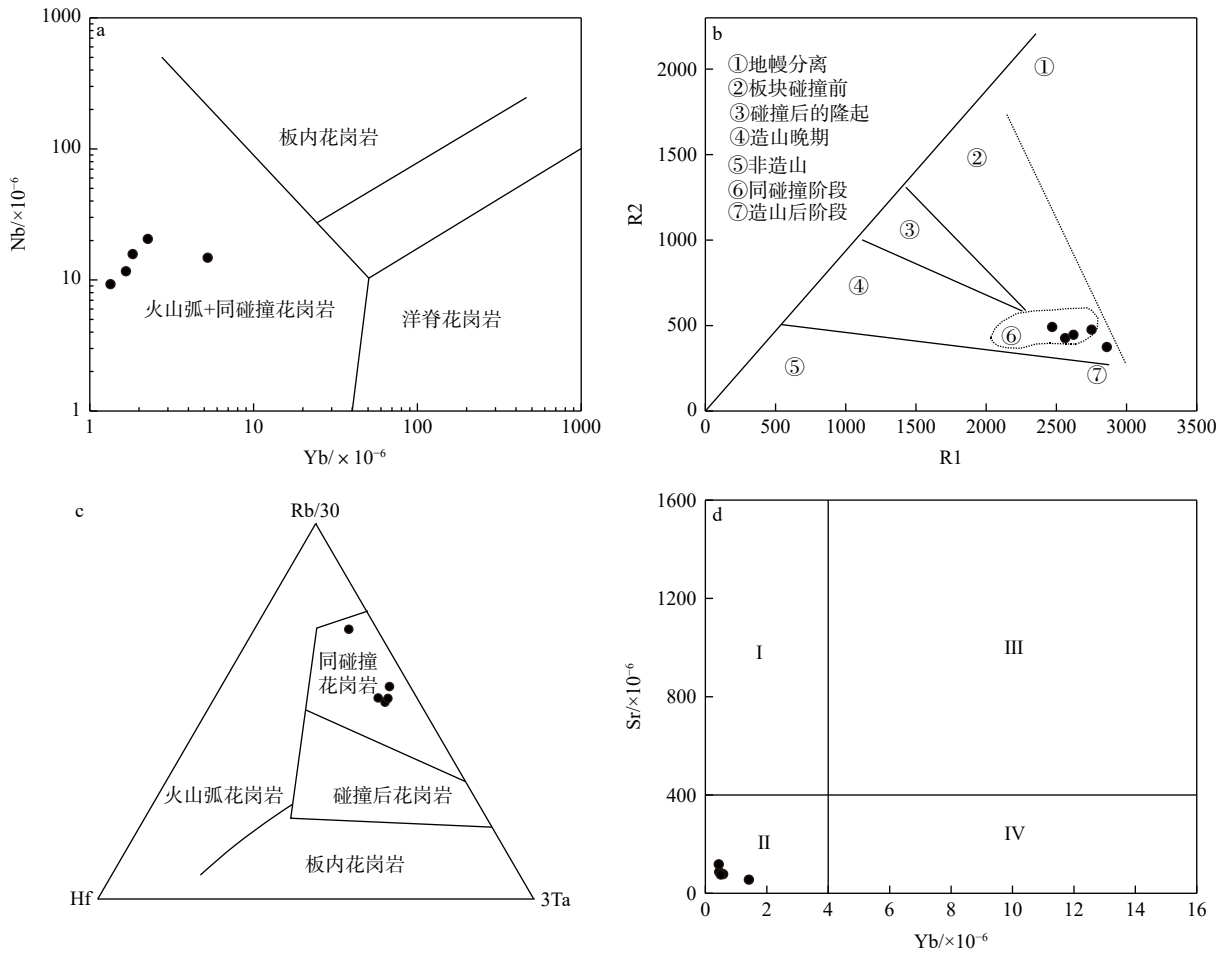
的高钾钙碱性、弱过铝质特征以及明显的 Eu 负异常, 进一步支持了其形成于陆内俯冲或板内变形的构造背景。与此同时, Lin et al. (2018) 提出了华南早古生代可能经历了多期次的板块俯冲和碰撞, 认为华南与冈瓦纳大陆北缘的相互作用可能是加里东期造山运动的主要驱动力。澜河岩体的稀土元素配分模式 (LREE/HREE 为 9.49~28.15, Eu 负异常明显) 与多期次俯冲碰撞模型中地壳物质部分熔融的特征一致, 这表明澜河岩体的形成可能同时受到内部构造重组和外部板块俯冲的影响。

综上所述, 澜河片麻状黑云母花岗岩的研究为华南早古生代构造演化提供了新的年代学和地球化学约束。结合区域地质资料, 澜河岩体可能是华南加里东期造山运动从挤压增厚向后碰撞伸展的转变的产物, 这一转变可能与华南内部的构造重组或外部板块的俯冲碰撞有关。

5 结论

(1) 澜河岩体片麻状黑云母花岗岩 LA-ICP-MS 锆石 U-Pb 同位素年龄为 427 ± 2 Ma, 属于加里东晚期岩浆活动的产物, 为高分异 I 型花岗岩, 主要由地壳变质砂岩和变质泥岩部分熔融形成, 可能是古元古代基底在新元古代-早古生代多期改造后的产物。

(2) 澜河岩体片麻状黑云母花岗岩形成于早古生代的同碰撞构造环境, 可能是华南加里东期造山



I—高 Sr 低 Yb 型; II—低 Sr 低 Yb 型; III—高 Sr 高 Yb 型; IV—低 Sr 高 Yb 型; V—非常低 Sr 高 Yb 型

a—Yb-Nb 图解 (Pearce et al., 1984); b—R1-R2 图解 (Batchelor and Bowden, 1985); c—Rb/30-Ta \times 3-Hf 图解 (Harris, 1986); d—Yb-Sr 图解 (张旗等, 2008).

图 11 澜河片麻状黑云母花岗岩构造环境判别图解

Fig. 11 Tectonic discrimination diagrams for the gneissic biotite granites from the Lanhe pluton

(a) Yb vs. Ta diagram (Pearce et al., 1984); (b) R1 vs. R2 diagram (Batchelor and Bowden, 1985); (c) Rb/30 vs. Ta \times 3-Hf diagram (Harris, 1986); (d) Yb vs. Sr diagram (Zhang et al., 2008).

I :high Sr, low Yb type; II :low Sr, low Yb type; III :high Sr, high Yb type; IV :low Sr, high Yb type; V :very low Sr, high Yb type

运动从挤压增厚向后碰撞伸展的转变的产物, 这一转变可能与华南内部的构造重组或外部板块的俯冲碰撞有关。

References

- ALTHERR R, HOLL A, HEGNER E, et al., 2000. High-potassium, calc-alkaline I-type plutonism in the European Variscides: northern Vosges (France) and northern Schwarzwald (Germany)[J]. *Lithos*, 50(1-3): 51-73.
- BATCHELOR R A, BOWDEN P, 1985. Petrogenetic interpretation of granitoid rock series using multicatic parameters[J]. *Chemical Geology*, 48(1-4): 43-55.
- BOUVIER A, VERVOORT J D, PATCHETT P J, 2008. The Lu-Hf and Sm-Nd isotopic composition of CHUR: constraints from unequilibrated chondrites and implications for the bulk composition of terrestrial planets[J]. *Earth and Planetary Science Letters*, 273(1-2): 48-57.
- CAI D W, TANG Y, ZHANG H, et al., 2017. Petrogenesis and tectonic setting of the Devonian Xiqin A-type granite in the northeastern Cathaysia Block, SE China[J]. *Journal of Asian Earth Sciences*, 141: 43-58.
- CAWOOD P A, ZHAO G C, YAO J L, et al., 2018. Reconstructing South China in Phanerozoic and Precambrian supercontinents[J]. *Earth-Science Reviews*, 186: 173-194.
- CHAPPELL B W, WHITE A J R, 1974. Two contrasting granite types[J]. *Pacific Geology*, 8: 173-174.
- CHAPPELL B W, WHITE A J R, 2001. Two contrasting granite types: 25 years later[J]. *Australian Journal of Earth Sciences*, 48(4): 489-499.
- CHARVET J, SHU L S, FAURE M, et al., 2010. Structural development of

- the Lower Paleozoic belt of South China: genesis of an intracontinental orogen[J]. *Journal of Asian Earth Sciences*, 39(4): 309-330.
- CHEN B L, GAO Y, WANG Y, et al., 2024. Denudation and preservation of the Changjiang uranium ore field in North Guangdong, China: revealed by apatite fission track thermochronology[J]. *Geotectonica et Metallogenia*, 48(5): 911-927. (in Chinese with English abstract)
- CHEN B L, PEI Y R, 2025. Analysis of ore-controlling structure of Lujing uranium ore field in Hunan-Jiangxi border[J]. *Acta Geologica Sinica*, 1-25. (in Chinese with English abstract)
- COLEMAN R G, PETERMAN Z E, 1975. Oceanic plagiogranite[J]. *Journal of Geophysical Research*, 80(8): 1099-1108.
- DENG F L, 1987. Isotopic geochronology of the southern Zhuguangshan granite batholith[J]. *Geochimica*, 16(2): 141-152. (in Chinese with English abstract)
- DENG P, REN J S, LING H F, et al., 2011. Yanshanian granite batholiths of southern Zhuguang mountain: SHRIMP zircon U-Pb dating and tectonic implications[J]. *Geological Review*, 57(6): 881-888. (in Chinese with English abstract)
- DENG P, REN J S, LING H F, et al., 2012. SHRIMP zircon U-Pb ages and tectonic implications for Indosinian granitoids of southern Zhuguangshan granitic composite, South China[J]. *Chinese Science Bulletin*, 57(13): 1542-1552.
- DOUCE A E P, HARRIS N, 1998. Experimental constraints on Himalayan anatexis[J]. *Journal of Petrology*, 39(4): 689-710.
- FENG S J, ZHAO K D, LING H F, et al., 2014. Geochronology, elemental and Nd-Hf isotopic geochemistry of Devonian A-type granites in central Jiangxi, South China: Constraints on petrogenesis and post-collisional extension of the Wuyi-Yunkai orogeny[J]. *Lithos*, 206-207: 1-18.
- GAO S, LUO T C, ZHANG B R, et al., 1999. Structure and composition of the continental crust in East China[J]. *Science in China Series D: Earth Sciences*, 42(2): 129-140.
- GRIFFIN W L, WANG X, JACKSON S E, et al., 2002. Zircon chemistry and magma mixing, SE China: in-situ analysis of Hf isotopes, Tonglu and Pingtan igneous complexes[J]. *Lithos*, 61(3-4): 237-269.
- GUAN Y L, YUAN C, SUN M, et al., 2014. I-type granitoids in the eastern Yangtze Block: implications for the Early Paleozoic intracontinental orogeny in South China[J]. *Lithos*, 206-207: 34-51.
- GUO C L, LIU Z K, 2021. Caledonian granites in South China: the geological and geochemical characteristics on their petrogenesis and mineralization[J]. *Journal of Earth Sciences and Environment*, 43(6): 927-961. (in Chinese with English abstract)
- HARRIS N B W, PEARCE J A, TINDLE A G, 1986. Geochemical characteristics of collision zone magmatism[J]. *Geological Society, London, Special Publications*, 19(1): 67-81.
- HU R Z, BI X W, SU W C, et al., 2004. The relationship between uranium metallogenesis and crustal extension during the Cretaceous-Tertiary in South China[J]. *Earth Science Frontiers*, 11(1): 153-160 (in Chinese with English abstract).
- HU R Z, BI X W, ZHOU M F, et al., 2008. Uranium metallogenesis in South China and its relationship to crustal extension during the cretaceous to tertiary[J]. *Economic Geology*, 103(3): 583-598.
- HU R Z, LUO J C, CHEN Y W, et al., 2019. Several progresses in the study of uranium deposits in South China[J]. *Acta Petrologica Sinica*, 35(9): 2625-2636. (in Chinese with English abstract).
- HUA R M, ZHANG W L, CHEN P R, et al., 2013. Relationship between Caledonian granitoids and large-scale mineralization in South China[J]. *Geological Journal of China Universities*, 19(1): 1-11. (in Chinese with English abstract)
- HUANG G L, CAO H J, LING H F, et al., 2012. Zircon SHRIMP U-Pb age, geochemistry and genesis of the Youdong granite in northern Guangdong[J]. *Acta Geologica Sinica*, 86(4): 577-586. (in Chinese with English abstract)
- HUANG G L, LIU X Y, SUN L Q, et al., 2014. Zircon U-Pb dating, geochemical characteristic and genesis of the Changjiang granite in northern Guangdong[J]. *Acta Geologica Sinica*, 88(5): 836-849. (in Chinese with English abstract)
- HUANG X L, YU Y, LI J, et al., 2013. Geochronology and petrogenesis of the early Paleozoic I-type granite in the Taishan area, South China: middle-lower crustal melting during orogenic collapse[J]. *Lithos*, 177: 268-284.
- Institute of Geochemistry, Chinese Academy of Sciences, Isotope Geochronology Laboratory, 1972. Study on isotopic ages of granites in the Nanling Mountains and adjacent regions[J]. *Geochemistry*, 1(2): 119-134.
- JENSEN B B, 1973. Patterns of trace element partitioning[J]. *Geochimica et Cosmochimica Acta*, 37(10): 2227-2242.
- KONG H, LI H, WU Q H, et al., 2018. Co-development of Jurassic I-type and A-type granites in southern Hunan, South China: Dual control by plate subduction and intraplate mantle upwelling[J]. *Geochemistry*, 78(4): 500-520.
- LI F R, PAN J Y, ZHONG F J, et al., 2025. Petrogenesis and uranium mineralization potential of granites of the Xiaoshan deposit in the Lujing uranium ore field, Jiangxi province[J]. *Geoscience*, 1-29. (in Chinese with English abstract)
- LI L M, LIN S F, XING G F, et al., 2022. Identification of ca. 520 Ma mid-ocean-ridge-type Ophiolite suite in the inner Cathaysia block, South China: evidence from shearing-type oceanic Plagiogranite[J]. *GSA Bulletin*, 134(7-8): 1701-1720.
- LI X H, 1993. On the genesis of caledonian granitoid rocks at Wanyangshan and Zhuguangshan, Southeast China: evidence from trace elements and rare-earth elements geochemistry[J]. *Geochimica*, 22(1): 35-44. (in Chinese with English abstract)
- LI X H, HU R Z, RAO B, 1997. Geochronology and geochemistry of cretaceous mafic dikes from northern Guangdong, se China[J]. *Geochimica*, 26(2): 14-31. (in Chinese with English abstract)
- LI X H, LI W X, LI Z X, et al., 2009. Amalgamation between the Yangtze and Cathaysia Blocks in South China: constraints from SHRIMP U-Pb zircon ages, geochemistry and Nd-Hf isotopes of the Shuangxiwu volcanic rocks[J]. *Precambrian Research*, 174(1-2): 117-128.
- LI X H, LI Z X, LI W X, 2014. Detrital zircon U-Pb age and Hf isotope constrains on the generation and reworking of Precambrian continental crust in the Cathaysia block, South China: a synthesis[J]. *Gondwana Research*, 25(3): 1202-1215.
- LI Z X, LI X H, WARTHO J A, et al., 2010. Magmatic and metamorphic events during the early Paleozoic Wuyi-Yunkai orogeny, southeastern

- South China: new age constraints and pressure–temperature conditions[J]. *GSA Bulletin*, 122(5-6): 772-793.
- LIN S F, XING G F, DAVIS D W, et al., 2018. Appalachian-style multi-terrane Wilson cycle model for the assembly of South China[J]. *Geology*, 46(4): 319-322.
- LIU M H, SHI Y, TANG Y L, et al., 2021. Petrogenesis and tectonic significance of Caledonian I-type Granitoids in southeast Guangxi, South China[J]. *Earth Science*, 46(11): 3965-3992. (in Chinese with English abstract)
- LIU S F, PENG S B, KUSKY T, et al., 2018. Origin and tectonic implications of an early Paleozoic (460-440Ma) subduction-accretion shear zone in the northwestern Yunkai Domain, South China[J]. *Lithos*, 322: 104-128.
- LIU Y D, SU X L, CHENG H Y, et al., 2022. Geochronological and geochemical characteristics of the Caledonian Longquan pluton in southern Zhejiang, and their geological significance[J]. *Journal of Geomechanics*, 28(2): 237-256. (in Chinese with English abstract)
- LOISELLE M C, WONES D R, 1979. Characteristics of anorogenic granites[J]. *Geological society of America, Abstracts with Programs*, 11: 468.
- LUDWIG K R, 2003. ISOPLOT 3.00: a geochronological toolkit for Microsoft excel[M]. Berkeley: Berkeley Geochronology Center: 1-70.
- MANIAR P D, PICCOLI P M, 1989. Tectonic discrimination of granitoids[J]. *GSA Bulletin*, 101(5): 635-643.
- MIDDLEMOST E A K, 1994. Naming materials in the magma/igneous rock system[J]. *Earth-Science Reviews*, 37(3-4): 215-224.
- NARDI L V S, FORMOSO M L L, MÜLLER I F, et al., 2013. Zircon/rock partition coefficients of REEs, Y, Th, U, Nb, and Ta in granitic rocks: Uses for provenance and mineral exploration purposes[J]. *Chemical Geology*, 335: 1-7.
- PEARCE J A, HARRIS N B W, TINDLE A G, 1984. Trace element discrimination diagrams for the tectonic interpretation of granitic rocks[J]. *Journal of Petrology*, 25(4): 956-983.
- PECCERILLO A, TAYLOR S R, 1976. Geochemistry of Eocene calc-alkaline volcanic rocks from the Kastamonu area, northern Turkey[J]. *Contributions to Mineralogy and Petrology*, 58(1): 63-81.
- PENG S B, JIN Z M, LIU Y H, et al., 2006. Petrochemistry, chronology and tectonic setting of strong peraluminous anatectic granitoids in Yunkai orogenic belt, western Guangdong province, China[J]. *Earth Science—Journal of China University of Geosciences*, 31(1): 110-120. (in Chinese with English abstract)
- PENG S B, LIU S F, LIN M S, et al., 2016a. Early Paleozoic subduction in Cathaysia (I): new evidence from Nuodong ophiolite[J]. *Earth Science*, 41(5): 765-778. (in Chinese with English abstract)
- PENG S B, LIU S F, LIN M S, et al., 2016b. Early Paleozoic subduction in Cathaysia (II): new evidence from the Dashuang high Magnesian-Magnesian andesite[J]. *Earth Science*, 41(6): 931-947. (in Chinese with English abstract)
- PLANK T, LANGMUIR C H, 1998. The chemical composition of subducting sediment and its consequences for the crust and mantle[J]. *Chemical Geology*, 145(3-4): 325-394.
- QIU X F, ZHAO X M, YANG H M, et al., 2018. Petrogenesis of the Early Palaeozoic granitoids from the Yunkai massif, South China block: implications for a tectonic transition from compression to extension during the Caledonian orogenic event[J]. *Geological Magazine*, 155(8): 1776-1792.
- SHU L S, 2006. Predevonian tectonic evolution of South China: from Cathaysian block to Caledonian period folded orogenic belt[J]. *Geological Journal of China Universities*, 12(4): 418-431. (in Chinese with English abstract)
- SHU L S, FAURE M, JIANG S Y, et al., 2006. SHRIMP zircon U-Pb age, litho- and biostratigraphic analyses of the Huaiyu domain in South China: Evidence for a Neoproterozoic orogen, not late Paleozoic-early Mesozoic collision[J]. *Episodes*, 29(4): 244-252.
- SHU L S, FAURE M, YU J H, et al., 2011. Geochronological and geochemical features of the Cathaysia block (South China): new evidence for the Neoproterozoic breakup of Rodinia[J]. *Precambrian Research*, 187(3-4): 263-276.
- SHU L S, 2012. An analysis of principal features of tectonic evolution in South China block[J]. *Geological Bulletin of China*, 31(7): 1035-1053. (in Chinese with English abstract)
- SHU L S, JAHN B M, CHARVET J, et al., 2014. Early Paleozoic depositional environment and intraplate tectono-magmatism in the Cathaysia Block (South China): Evidence from stratigraphic, structural, geochemical and geochronological investigations[J]. *American Journal of Science*, 314(1): 154-186.
- SHU L S, WANG B, CAWOOD P A, et al., 2015. Early Paleozoic and early Mesozoic intraplate tectonic and magmatic events in the Cathaysia block, South China[J]. *Tectonics*, 34(8): 1600-1621.
- SHU L S, SONG M J, YAO J L, 2018. Appalachian-style multi-terrane Wilson cycle model for the assembly of South China: COMMENT[J]. *Geology*, 46(6): e445.
- SHU L S, CHEN X Y, LOU F S, 2020. Pre-Jurassic tectonics of the South China[J]. *Acta Geologica Sinica*, 94(2): 333-360. (in Chinese with English abstract)
- SLÁMA J, KOŠLER J, CONDON D J, et al., 2008. Plešovice zircon—a new natural reference material for U-Pb and Hf isotopic microanalysis[J]. *Chemical Geology*, 249(1-2): 1-35.
- SÖDERLUND J, 2004. Building theories of project management: past research, questions for the future[J]. *International Journal of Project Management*, 22(3): 183-191.
- SUN S S, MCDONOUGH W F, 1989. Chemical and isotopic systematics of oceanic basalts: implications for mantle composition and processes[J]. *Geological Society, London, Special Publications*, 42(1): 313-345.
- SUN T, 2006. A new map showing the distribution of granites in South China and its explanatory notes[J]. *Geological Bulletin of China*, 25(3): 332-335. (in Chinese with English abstract)
- SYLVESTER P J, 1998. Post-collisional strongly peraluminous granites[J]. *Lithos*, 45(1-4): 29-44.
- TAYLOR S R, MCLENNAN S M, 1985. The continental crust: its composition and evolution[M]. Oxford: Blackwell Scientific Publications: 312.
- WANG L J, ZHANG K X, LIN S F, et al., 2022. Origin and age of the Shenshan tectonic mélange in the Jiangshan-Shaoxing-Pingxiang fault and late early Paleozoic juxtaposition of the Yangtze block and the West Cathaysia Terrane, South China[J]. *GSA Bulletin*, 134(1-2): 113-129.

- WANG L J, LIN S F, XIAO W J, 2023. Yangtze and Cathaysia blocks of South China: their separate positions in Gondwana until early Paleozoic juxtaposition[J]. *Geology*, 51(8): 723-727.
- WANG L J, LIN S F, XIAO W J, et al., 2024. Identifying and characterizing missing source Orogens for Syn-Orogenic basins based on detrital accessory mineral U-Pb geochronology and trace element geochemistry[J]. *Geology*, 52(8): 577-582.
- WANG L K, ZHANG Y Q, LIU S X, 1975. Multiple emplacements and some geochemical characteristics of the Zhuguangshan granitic batholith, Southern China[J]. *Geochimica*, 4(3): 189-201. (in Chinese with English abstract)
- WANG L L, 2015. Geochemistry and petrogenesis of early Paleozoic-Mesozoic granites in Ganzhou, Jiangxi Province, South China block[D]. Beijing: China University of Geosciences (Beijing). (in Chinese with English abstract)
- WANG X L, ZHOU J C, GRIFIIN W L, et al., 2014. Geochemical zonation across a Neoproterozoic orogenic belt: isotopic evidence from granitoids and metasedimentary rocks of the Jiangnan orogen, China[J]. *Precambrian Research*, 242: 154-171.
- WANG Y J, ZHANG A M, FAN W M, et al., 2011. Kwangian crustal anatexis within the eastern South China Block: geochemical, zircon U-Pb geochronological and Hf isotopic fingerprints from the gneissoid granites of Wugong and Wuyi-Yunkai domains[J]. *Lithos*, 127(1-2): 239-260.
- WANG Y J, FAN W M, ZHANG G W, et al., 2013. Phanerozoic tectonics of the South China block: key observations and controversies[J]. *Gondwana Research*, 23(4): 1273-1305.
- WATSON E B, HARRISON T M, 1983. Zircon saturation revisited: temperature and composition effects in a variety of crustal magma types[J]. *Earth and Planetary Science Letters*, 64(2): 295-304.
- WHALEN J B, CURRIE K L, CHAPPELL B W, 1987. A-type granites: geochemical characteristics, discrimination and petrogenesis[J]. *Contributions to Mineralogy and Petrology*, 95(4): 407-419.
- WIEDENBECK MAPC, ALLÉ P, CORFU F, et al., 1995. Three natural zircon standards for U-Th-Pb, Lu-Hf, trace element and REE analyses[J]. *Geostandards Newsletter*, 19(1): 1-23.
- WU F Y, LI X H, YANG J H, et al., 2007. Discussions on the petrogenesis of granites[J]. *Acta Petrologica Sinica*, 23(6): 1217-1238. (in Chinese with English abstract)
- WU Y B, ZHENG Y F, 2004. Genesis of zircon and its constraints on interpretation of U-Pb age[J]. *Chinese Science Bulletin*, 49(15): 1554-1569.
- XIA Y, XU X S, NIU Y L, et al., 2018. Neoproterozoic amalgamation between Yangtze and Cathaysia blocks: the magmatism in various tectonic settings and continent-arc-continent collision[J]. *Precambrian Research*, 309: 56-87.
- XIN Y J, LI J H, RATSCHBACHER L, et al., 2020. Early Devonian (415-400 Ma) a-type granitoids and diabases in the Wuyishan, eastern Cathaysia: a signal of crustal extension coeval with the separation of South China from Gondwana[J]. *GSA Bulletin*, 132(11-12): 2295-2317.
- XU W J, XU X S, 2015. Early Paleozoic intracontinental felsic magmatism in the South China Block: petrogenesis and geodynamics[J]. *Lithos*, 234-235: 79-92.
- XU W J, 2017. The petrogenesis of early Paleozoic intracontinental magmatism in the Zhuguang-Wanyang Mts district, Cathaysia block[D]. Nanjing: Nanjing University. (in Chinese with English abstract)
- XU Y J, CAWOOD P A, DU Y S, 2016. Intraplate orogenesis in response to Gondwana Assembly: Kwangian Orogeny, South China[J]. *American Journal of Science*, 316(4): 329-362.
- YU J H, O'REILLY S Y, WANG L J, et al., 2010. Components and episodic growth of Precambrian crust in the Cathaysia Block, South China: evidence from U-Pb ages and Hf isotopes of zircons in Neoproterozoic sediments[J]. *Precambrian Research*, 181(1-4): 97-114.
- ZHANG F F, WANG Y J, ZHANG A M, et al., 2012. Geochronological and geochemical constraints on the Petrogenesis of middle Paleozoic (Kwangian) massive granites in the eastern South China block[J]. *Lithos*, 150: 188-208.
- ZHANG F R, SHU L S, WANG D Z, et al., 2009. Discussions on the tectonic setting of Caledonian granitoids in the eastern segment of South China[J]. *Earth Science Frontiers*, 16(1): 248-260. (in Chinese with English abstract)
- ZHANG F R, 2011. The geological and geochemical characteristics and its Petrogenesis for Caledonian granites in the central-southern Jiangxi Province[D]. Nanjing: Nanjing University. (in Chinese with English abstract)
- ZHANG L, CHEN Z Y, LI S R, et al., 2017. Isotope geochronology, geochemistry, and mineral chemistry of the U-bearing and barren granites from the Zhuguangshan Complex, South China: implications for petrogenesis and Uranium Mineralization[J]. *Ore Geology Reviews*, 91: 1040-1065.
- ZHANG L, CHEN Z Y, LI X F, et al., 2018. Zircon U-Pb geochronology and geochemistry of granites in the Zhuguangshan Complex, South China: Implications for uranium mineralization[J]. *Lithos*, 308-309: 19-33.
- ZHANG L, CHEN Z Y, WANG F Y, et al., 2021. Apatite geochemistry as an indicator of petrogenesis and uranium fertility of granites: A case study from the Zhuguangshan batholith, South China[J]. *Ore Geology Reviews*, 128: 103886.
- ZHANG Q, WANG Y L, JIN W J, et al., 2008. Criteria for the recognition of pre-, syn- and post-orogenic granitic rocks[J]. *Geological Bulletin of China*, 27(1): 1-18. (in Chinese with English abstract)
- ZHANG Q, JIANG Y H, WANG G C, et al., 2015. Origin of Silurian gabbros and I-type granites in Central Fujian, SE China: implications for the evolution of the Early Paleozoic orogen of South China[J]. *Lithos*, 216-217: 285-297.
- ZHANG S M, 2023. Characteristics, genesis and tectonic significance of the Zhuguangshan composite batholith, South China[D]. Beijing: Chinese Academy of Geological Sciences. (in Chinese with English abstract)
- ZHAO L, GUO F, ZHANG X B, et al., 2021. Cretaceous crustal melting records of tectonic transition from subduction to slab rollback of the Paleopacific Plate in SE China[J]. *Lithos*, 384-385: 105985.
- ZHONG Y F, WANG L X, ZHAO J H, et al., 2016. Partial melting of an ancient sub-continental lithospheric mantle in the Early Paleozoic intracontinental regime and its contribution to petrogenesis of the coeval peraluminous granites in South China[J]. *Lithos*, 264: 224-238.
- ZHOU H B, PAN J Y, ZHONG F J, et al., 2018. Genesis of fine grained biotite granite in the Changjiang uranium ore field, northern Guangdong of

China, and its relation with uranium mineralization[J]. *Journal of Mineralogy and Petrology*, 38(1): 10-19. (in Chinese with English abstract)

ZHU B, 2010. The study of mantle liquid and uranium metallogenesis-take uranium ore field of south Zhuguang mountain as an example[D]. Chengdu: Chengdu University of Technology: 31-57. (in Chinese with English abstract)

附中文参考文献

陈柏林, 高允, 王永, 等, 2024. 粤北长江铀矿田隆升剥露历史和矿床保存: 来自磷灰石裂变径迹热年代学的启示[J]. *大地构造与成矿学*, 48(5): 911-927.

陈柏林, 裴英茹, 2025. 湘赣边界鹿井铀矿田控矿构造解析[J/OL]. *地质学报*, 1-25.

邓访陵, 1987. 诸广山花岗岩复式岩基南部的同位素地质年代学[J]. *地球化学*, 16(2): 141-152.

邓平, 任纪舜, 凌洪飞, 等, 2011. 诸广山南体燕山期花岗岩的锆石 SHRIMP U-Pb 年龄及其构造意义[J]. *地质论评*, 57(6): 881-888.

邓平, 任纪舜, 凌洪飞, 等, 2012. 诸广山南体印支期花岗岩的 SHRIMP 锆石 U-Pb 年龄及其构造意义[J]. *科学通报*, 57(14): 1231-1241.

高山, 骆庭川, 张本仁, 等, 1999. 中国东部地壳的结构和组成[J]. *中国科学(D辑)*, 29(3): 204-213.

郭春丽, 刘泽坤, 2021. 华南地区加里东期花岗岩: 成岩和成矿作用的地质与地球化学特征[J]. *地球科学与环境学报*, 43(6): 927-961.

胡瑞忠, 毕献武, 苏文超, 等, 2004. 华南白垩—第三纪地壳拉张与铀成矿的关系[J]. *地学前缘*, 2004, 11(1): 153-160.

胡瑞忠, 骆金诚, 陈佑伟, 等, 2019. 华南铀矿床研究若干进展[J]. *岩石学报*, 35(9): 2625-2636.

华仁民, 张文兰, 陈培荣, 等, 2013. 初论华南加里东花岗岩与大规模成矿作用的关系[J]. *高校地质学*, 19(1): 1-11.

黄国龙, 曹豪杰, 凌洪飞, 等, 2012. 粤北油洞岩体 SHRIMP 锆石 U-Pb 年龄、地球化学特征及其成因研究[J]. *地质学报*, 86(4): 57-586.

黄国龙, 刘鑫扬, 孙立强, 等, 2014. 粤北长江岩体的锆石 U-Pb 定年、地球化学特征及其成因研究[J]. *地质学报*, 88(5): 836-849.

李芙蓉, 潘家永, 钟福军, 等, 2025. 江西鹿井铀矿田小山矿床花岗岩成因及产铀潜力分析[J/OL]. *现代地质*, 1-29.

李献华, 1993. 万洋山—诸广山加里东期花岗岩的形成机制: 微量元素和稀土元素地球化学证据[J]. *地球化学*, 22(1): 35-44.

李献华, 胡瑞忠, 饶冰, 1997. 粤北白垩纪基性岩脉的年代学和地球化学[J]. *地球化学*, 26(2): 14-31.

刘明辉, 时毓, 唐远兰, 等, 2021. 华南桂东南地区加里东期 I 型花岗岩类的岩石成因及构造意义[J]. *地球科学*, 46(11): 3965-3992.

刘远栋, 苏小浪, 程海艳, 等, 2022. 浙南加里东期龙泉岩体年代学、地球化学特征及其地质意义[J]. *地质力学学报*, 28(2): 237-256.

彭松柏, 金振民, 刘云华, 等, 2006. 云开造山带强过铝深熔花岗岩地球化学、年代学及构造背景[J]. *地球科学——中国地质大学学报*, 31(1): 110-120.

彭松柏, 刘松峰, 林木森, 等, 2016a. 华夏早古生代俯冲作用(I): 来自糯垌蛇绿岩的新证据[J]. *地球科学*, 41(5): 765-778.

彭松柏, 刘松峰, 林木森, 等, 2016b. 华夏早古生代俯冲作用(II): 大爽高镁—镁质安山岩新证据[J]. *地球科学*, 41(6): 931-947.

舒良树, 2006. 华南前泥盆纪构造演化: 从华夏地块到加里东期造山带[J]. *高校地质学报*, 12(4): 418-431.

舒良树, 2012. 华南构造演化的基本特征[J]. *地质通报*, 31(7): 1035-1053.

舒良树, 陈祥云, 楼法生, 2020. 华南前侏罗纪构造[J]. *地质学报*, 94(2): 333-360.

孙涛, 2006. 新编华南花岗岩分布图及其说明[J]. *地质通报*, 25(3): 332-335.

王丽丽, 2015. 华南赣州地区早古生代晚期—中生代花岗岩类地球化学与岩石成因[D]. 北京: 中国地质大学(北京).

王联魁, 张玉泉, 刘师先, 1975. 南岭诸广山花岗岩体的多次侵入活动和某些地球化学特征[J]. *地球化学*, 4(3): 189-201.

吴福元, 李献华, 杨进辉, 等, 2007. 花岗岩成因研究的若干问题[J]. *岩石学报*, 23(6): 1217-1238.

徐文景, 2017. 华夏地块诸广—万洋山地区早古生代陆内岩浆作用与岩石成因[D]. 南京: 南京大学.

张芳荣, 舒良树, 王德滋, 等, 2009. 华南东段加里东期花岗岩类形成构造背景探讨[J]. *地学前缘*, 16(1): 248-260.

张芳荣, 2011. 江西中—南部加里东期花岗岩地质地球化学特征及其成因[D]. 南京: 南京大学.

张旗, 王元龙, 金惟俊, 等, 2008. 造山前、造山和造山后花岗岩的识别[J]. *地质通报*, 27(1): 1-18.

张素梅, 2023. 华南诸广山复式岩基的特征、成因及构造意义[D]. 北京: 中国地质科学院.

中国科学院贵阳地球化学研究所同位素年龄实验室, 湖北地质科学研究所同位素年龄实验室, 1972. 南岭及其邻区花岗岩同位素年龄的研究[J]. *地球化学*, 1(2): 119-134.

周航兵, 潘家永, 钟福军, 等, 2018. 粤北长江铀矿田细粒黑云母花岗岩的成因及其与铀成矿关系[J]. *矿物岩石*, 38(1): 10-19.

朱捌, 2010. 地幔流体与铀成矿作用研究: 以诸广山南部铀矿田为例[D]. 成都: 成都理工大学: 31-57.

开放科学 (资源服务) 标识码 (OSID):

可扫码查看澜河岩体及南岭加里东期岩体花岗岩锆石 Hf 同位素数据, 下载文章电子版, 听作者的语音介绍及更多文章相关资讯

